THE Attenuation Characteristic In Arc-continent Collision Zone Of Taiwan From Shallow To Deep

王郁如
Yu-Ju Wang

國立中央大學 地球科學系
中央研究院 地球科學研究所

outlines

* Introduction : Attenuation (Q^{-1})
* The attenuation properties of the Taiwan orogenic structure
* The attenuation features within the Chelungpu fault zone
* The subsurface attenuation model of Taiwan (depth ~300 m)
* New Attenuation Relationship for normal faulting earthquakes in the northeast offshore Taiwan

seismic attenuation (Q^{-1})

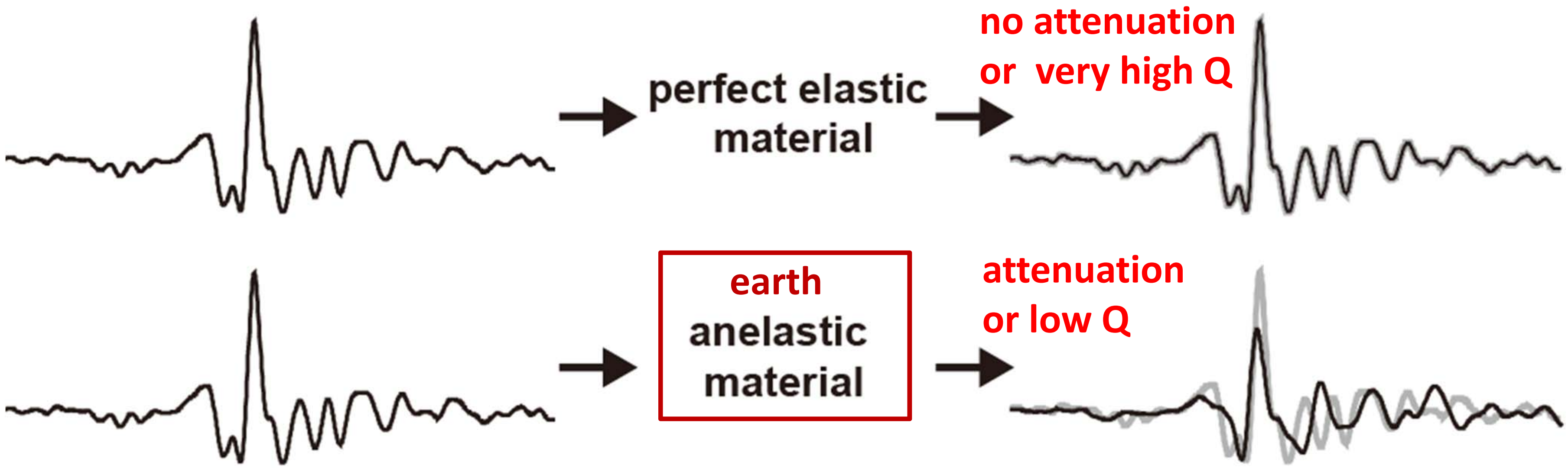

- Time domain: amplitude decay, longer duration
- Frequency domain: amplitude decay at high frequency
- Factors: temperature, fluid, cracks, permeability

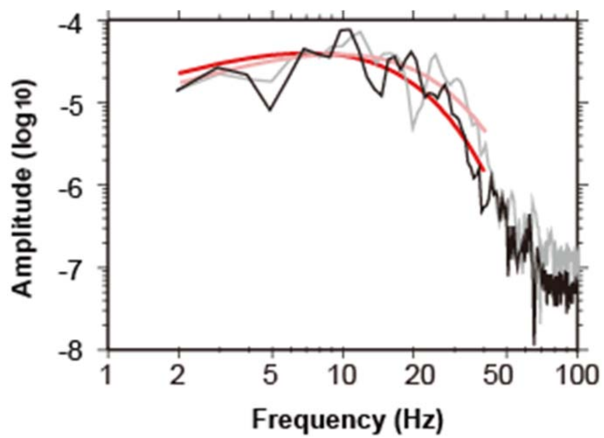

Subduction zone/volcanoes

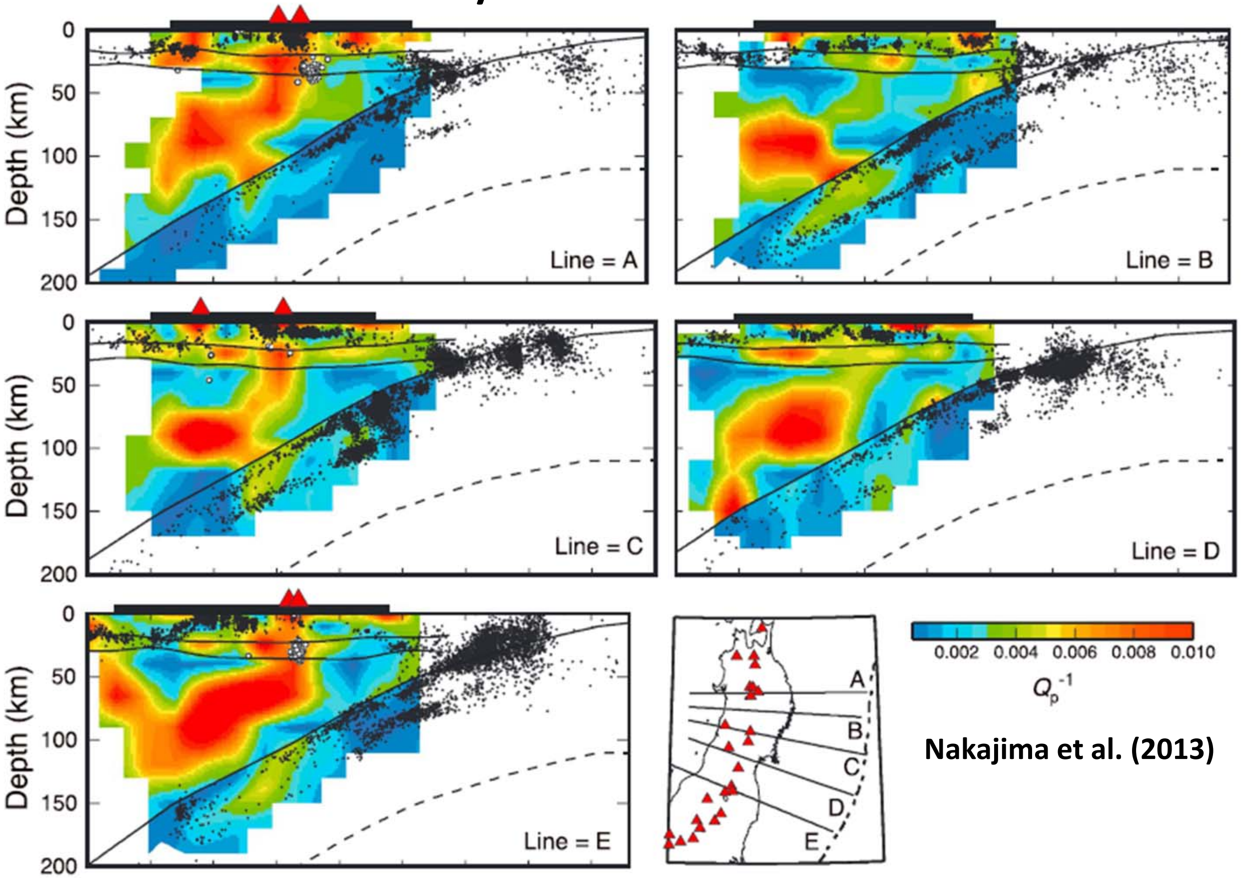

Nakajima et al. (2013)

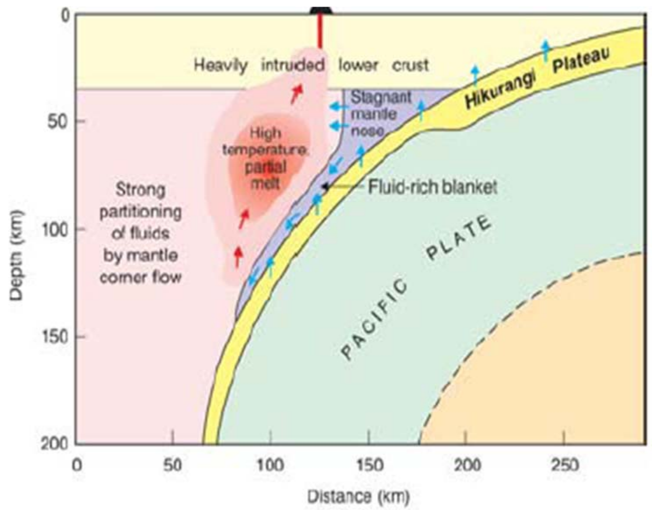

Eberhart-Phillips et al. (2009)

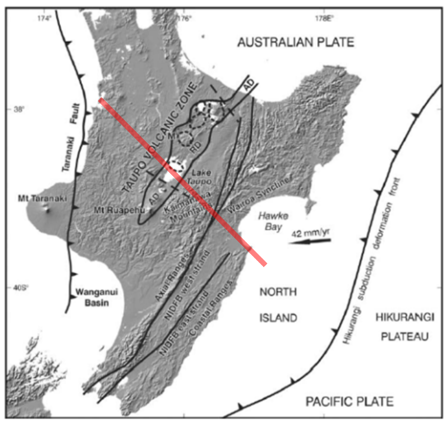

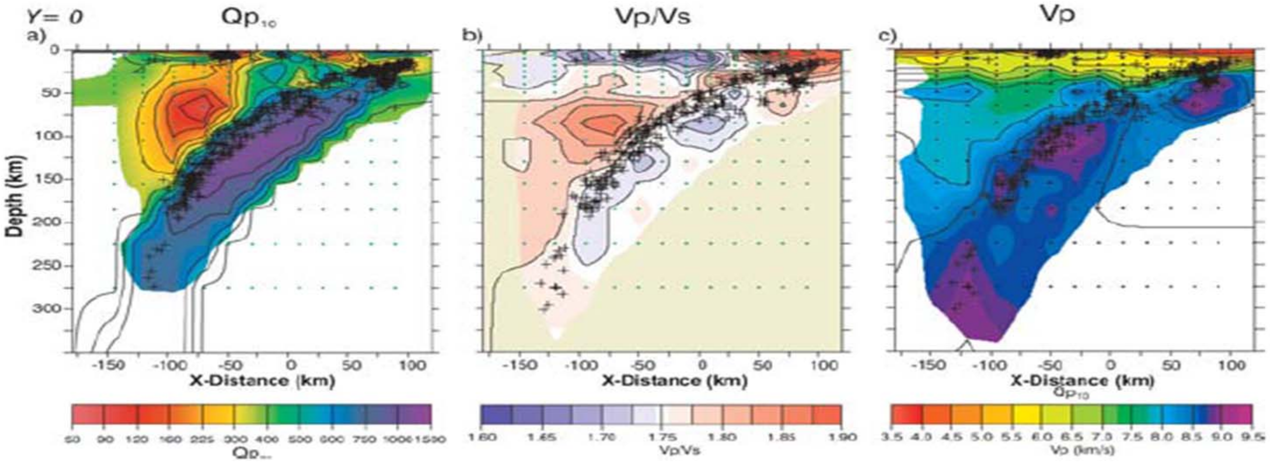

fault zone

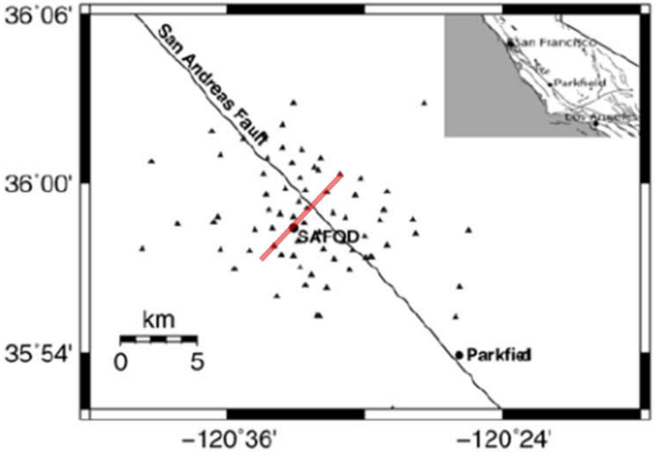

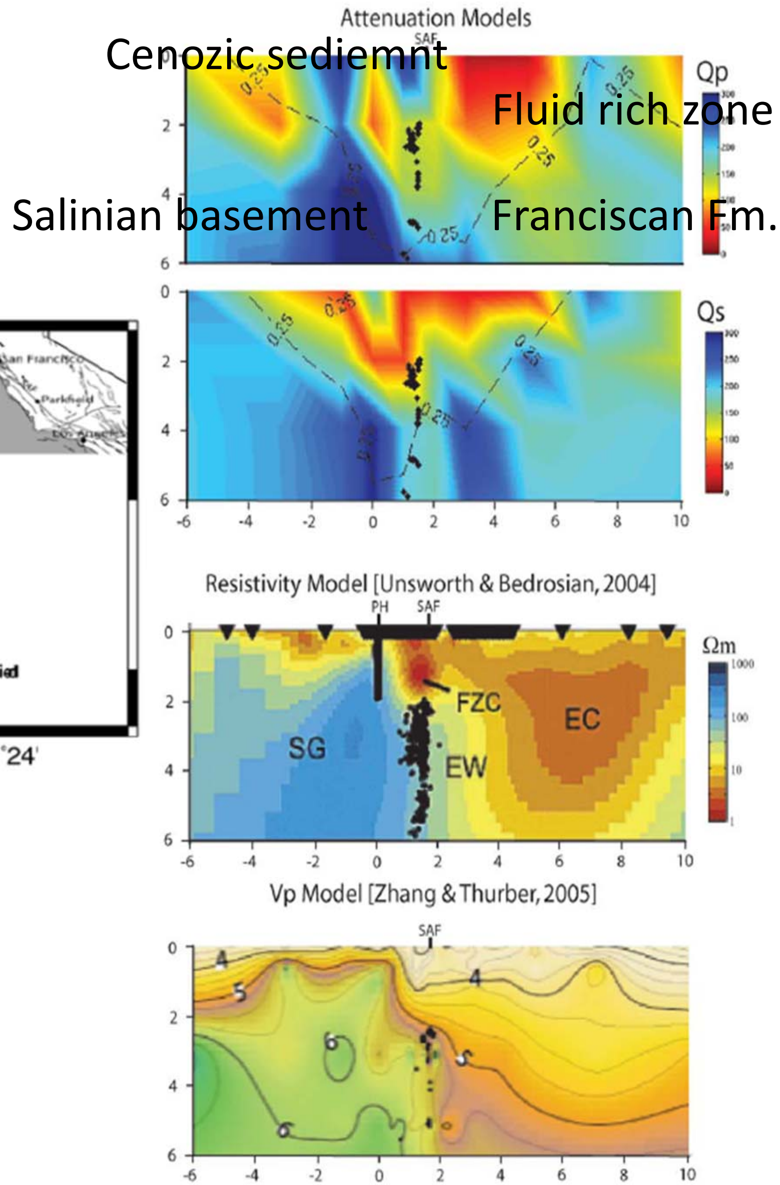

Bennington et al. (2008)

resource exploration

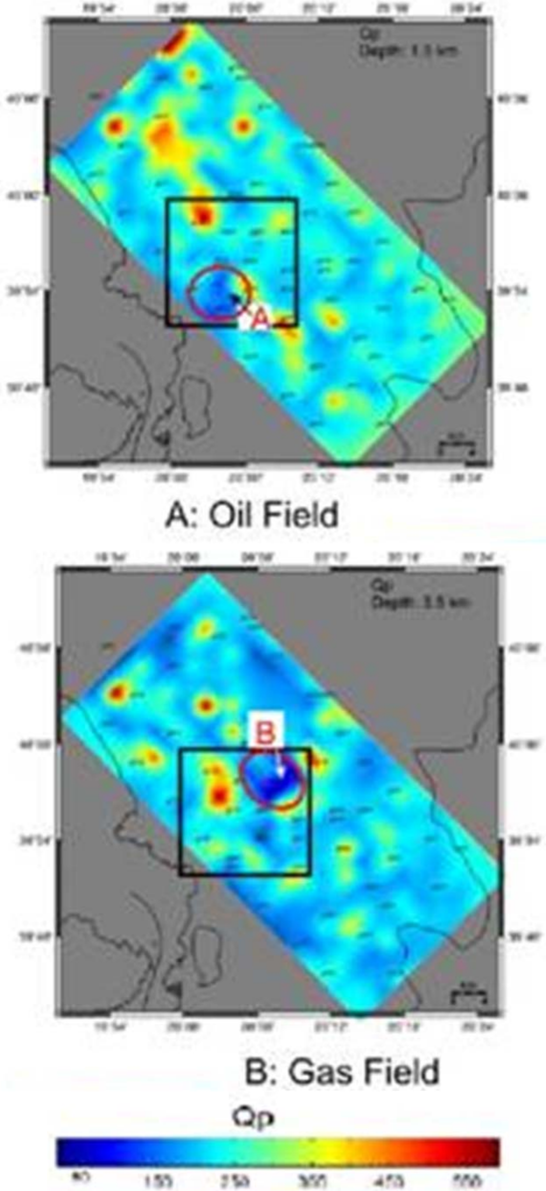

http://www.landtechsa.com

The attenuation properties of the Taiwan orogenic structure

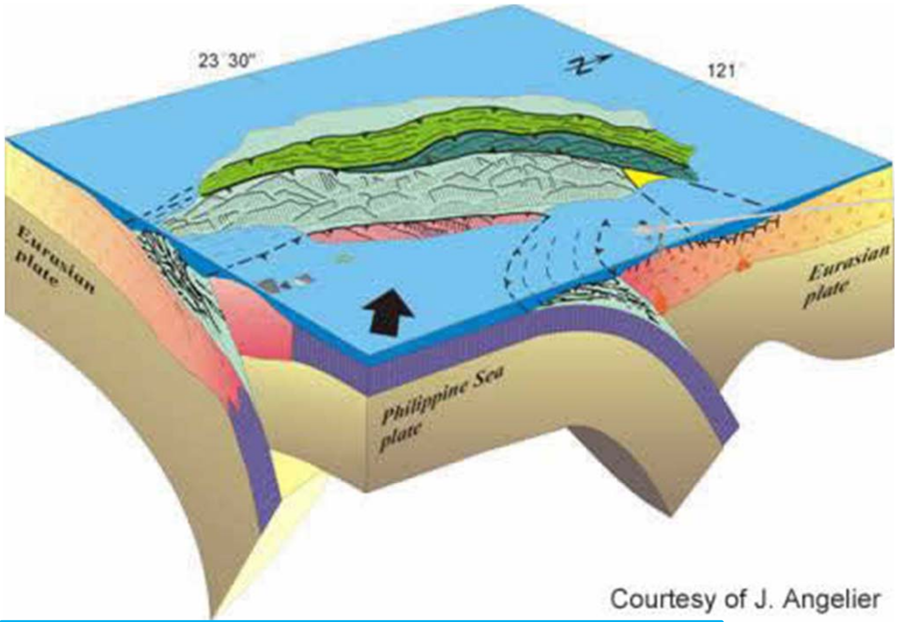

Courtesy of J. Angelier

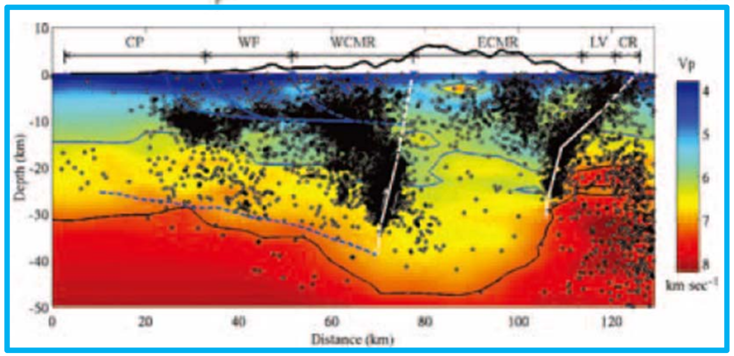

Kim et al. (2005)

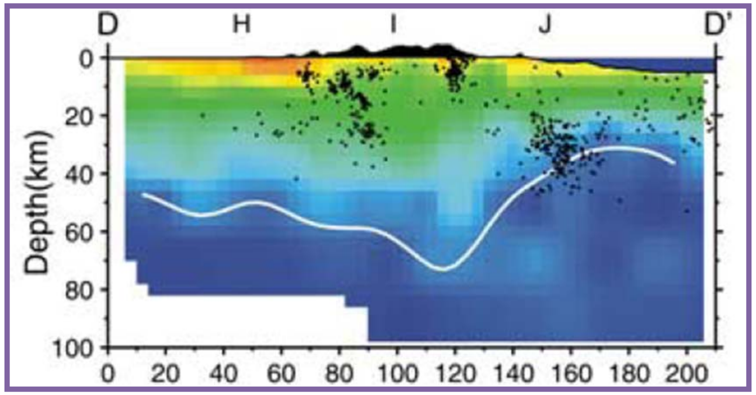

Wu et al. (2007)

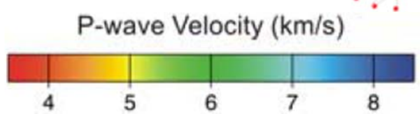

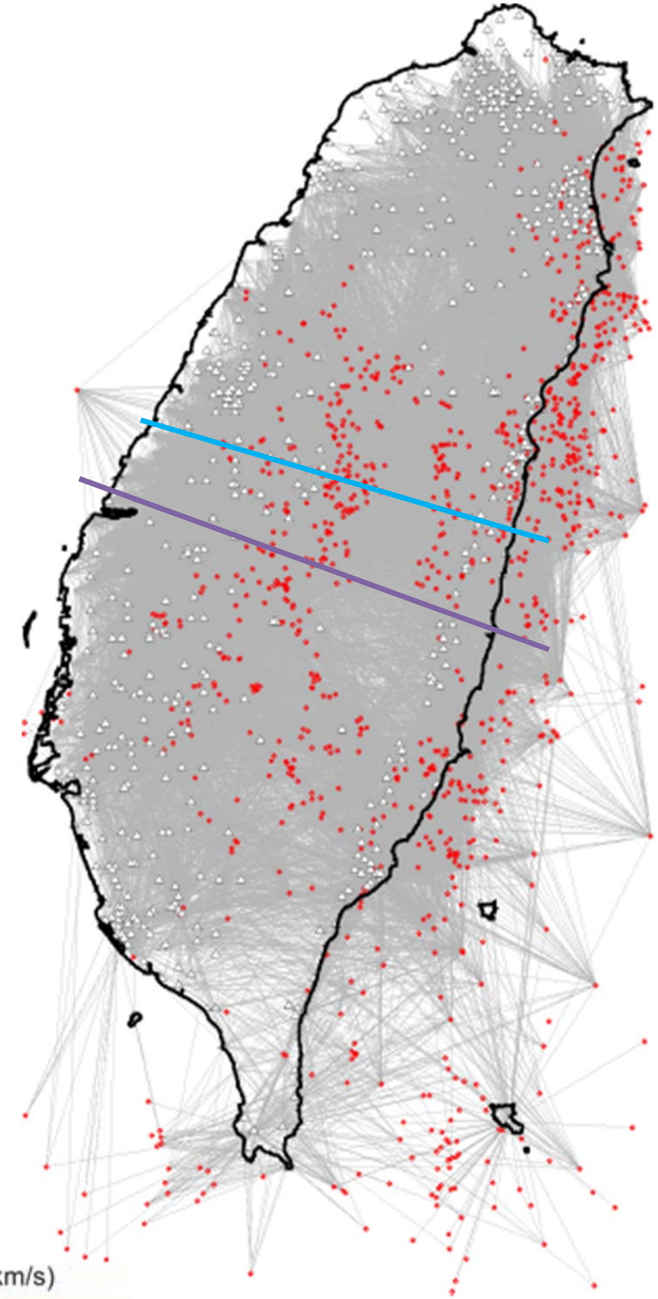

Wang et al. (2010)

Q tomography

- ***Observed velocity Spectrum:***

$$A_{ij}(f)=S_i(f)B_{ij}(f)R_j(f)I_j(f)$$

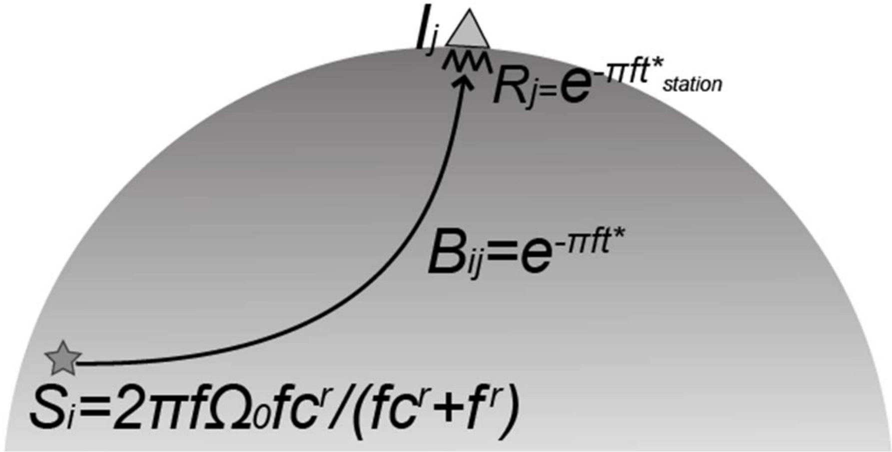

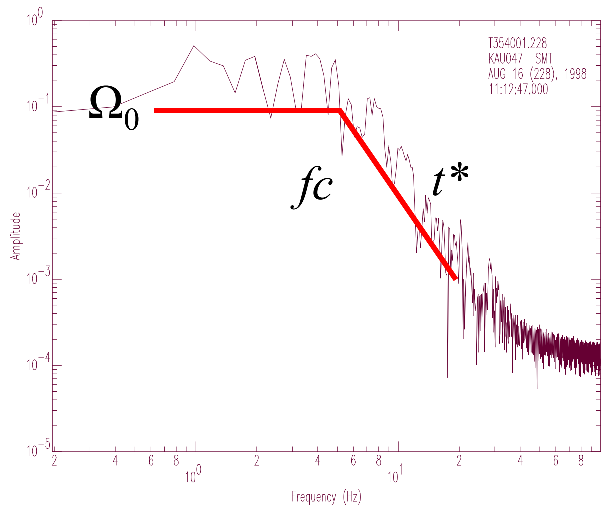

- ***ω^2-source model assumption:***

$$A_{ij}(f)=2\pi f\Omega_0 \frac{f_c^2}{f_c^2+f^2} e^{\ \pi f t^*}$$

(Eberhart-Phillips & Chadwick, 2002)

- ***Q tomography:***

$$t^* = \int_{source}^{receiver} \frac{1}{Q(s)V(s)} ds$$

fc : corner frequency
Ω_0:spectrum plateau value
t : whole-path attenuation operator*

Short-term average (STA) over long-term average (LTA) auto-picking algorithm

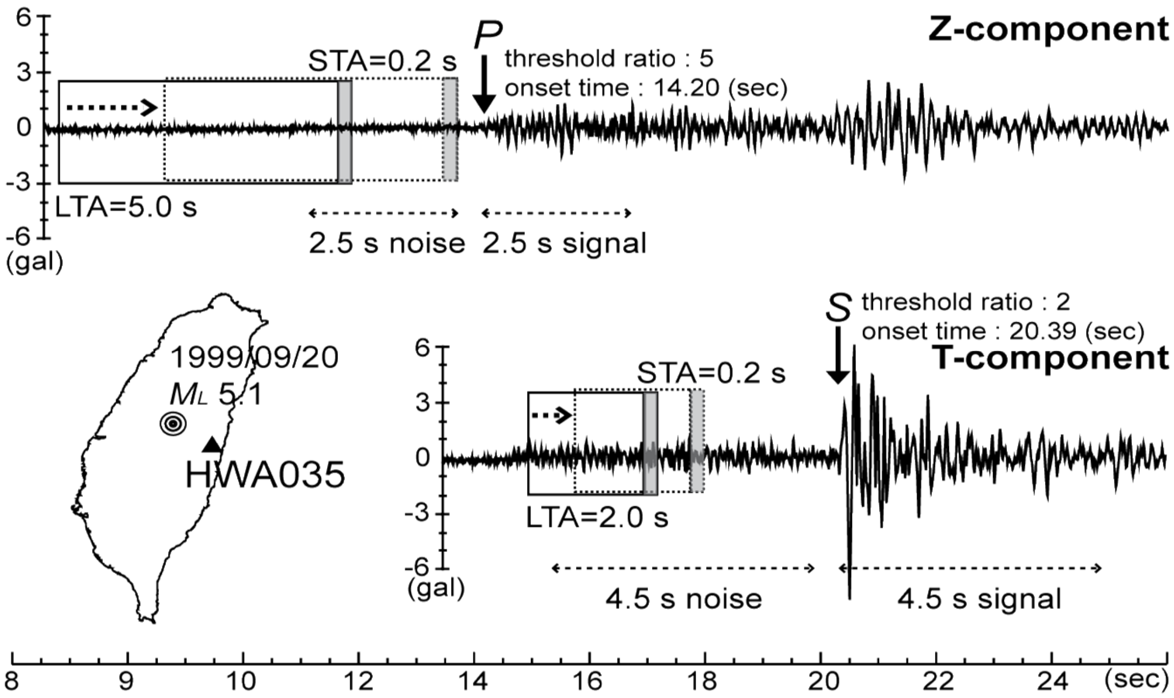

FFT

Data Quality Control

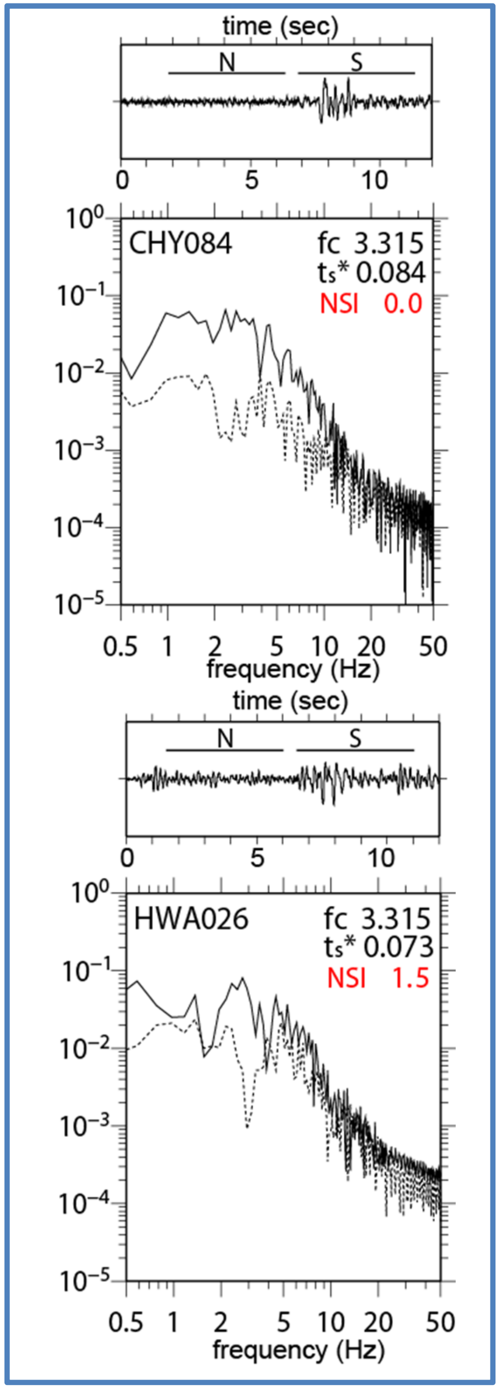

Quality	*D*: duration in 2–30 Hz of signal-to-noise ratio > 4.5 for Qp (in 1–20 Hz of signal-to-noise ratio > 2.3 for Qs)	NSI
Best	$D \geq 80$ per cent	0.0
	80 per cent > $D \geq 70$ per cent	0.5
↓	70 per cent > $D \geq 60$ per cent	1.0
	60 per cent > $D \geq 40$ per cent	1.5
Bad	40 per cent > D	2.0

two-steps of non-linear least-squares spectrum fitting

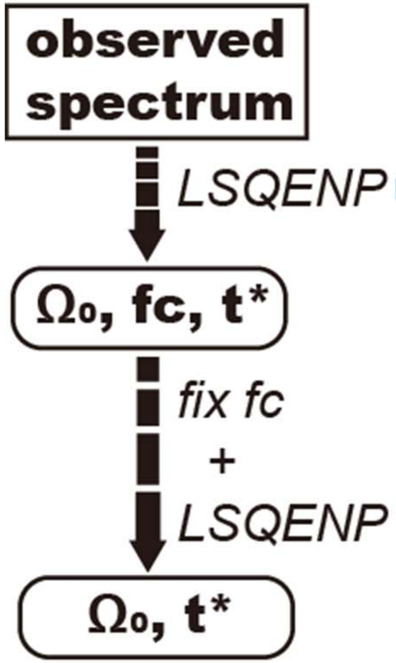

$$A_{ij}(f) = 2\pi f \Omega_0 \frac{f_c^2}{f_c^2 + f^2} e^{\pi f t^*}$$

$$\hat{Y}_i = f_i(X_i; b_1, b_2, b_3)$$

$$\frac{\partial \sum_{i=1}^{n} [Y_i - \langle Y_i \rangle]^2}{\partial d_j} = 0$$

$$\begin{bmatrix} Y_1 - f_1 \\ Y_2 - f_2 \\ \vdots \\ Y_n - f_n \end{bmatrix} = \begin{bmatrix} \frac{\partial f_1}{\partial b_1} & \frac{\partial f_1}{\partial b_2} & \frac{\partial f_1}{\partial b_3} \\ \frac{\partial f_2}{\partial b_1} & \frac{\partial f_2}{\partial b_2} & \frac{\partial f_2}{\partial b_3} \\ \vdots & \vdots & \vdots \\ \frac{\partial f_n}{\partial b_1} & \frac{\partial f_n}{\partial b_2} & \frac{\partial f_n}{\partial b_3} \end{bmatrix} \begin{bmatrix} b_1 - \hat{b}_1 \\ b_2 - \hat{b}_2 \\ b_3 - \hat{b}_3 \end{bmatrix}$$

$$B \quad = \quad P \quad \cdot \quad \vec{d}$$

$$P^T P \vec{d} - P^T B = 0$$

$$\vec{d} = (P^T P)^{-1} P^T B$$

$\hat{Y}$: predicted amplitude
X : frequency points
b_1 : Ω_0
b_2 : fc
b_3 : t^*

considering residual

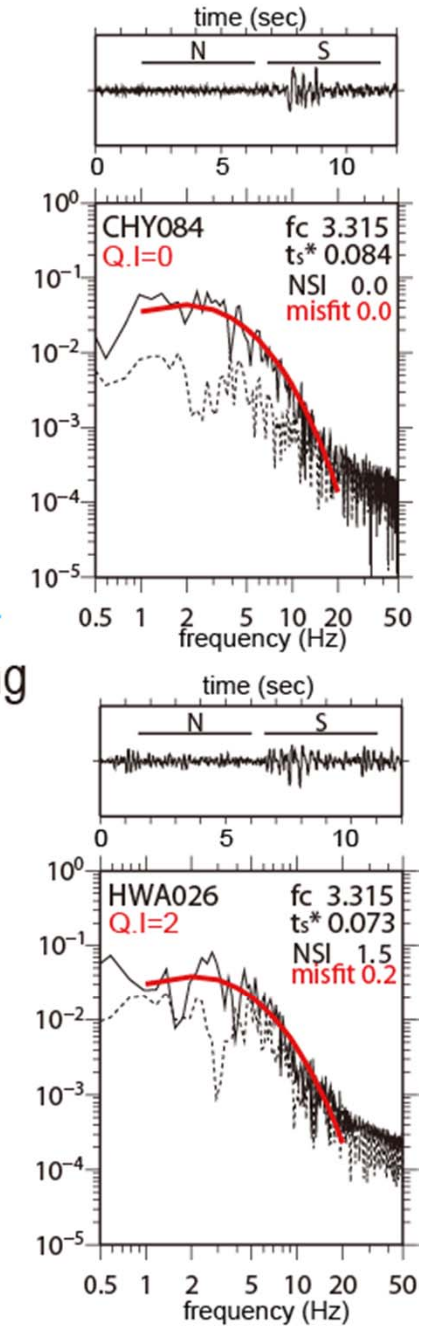

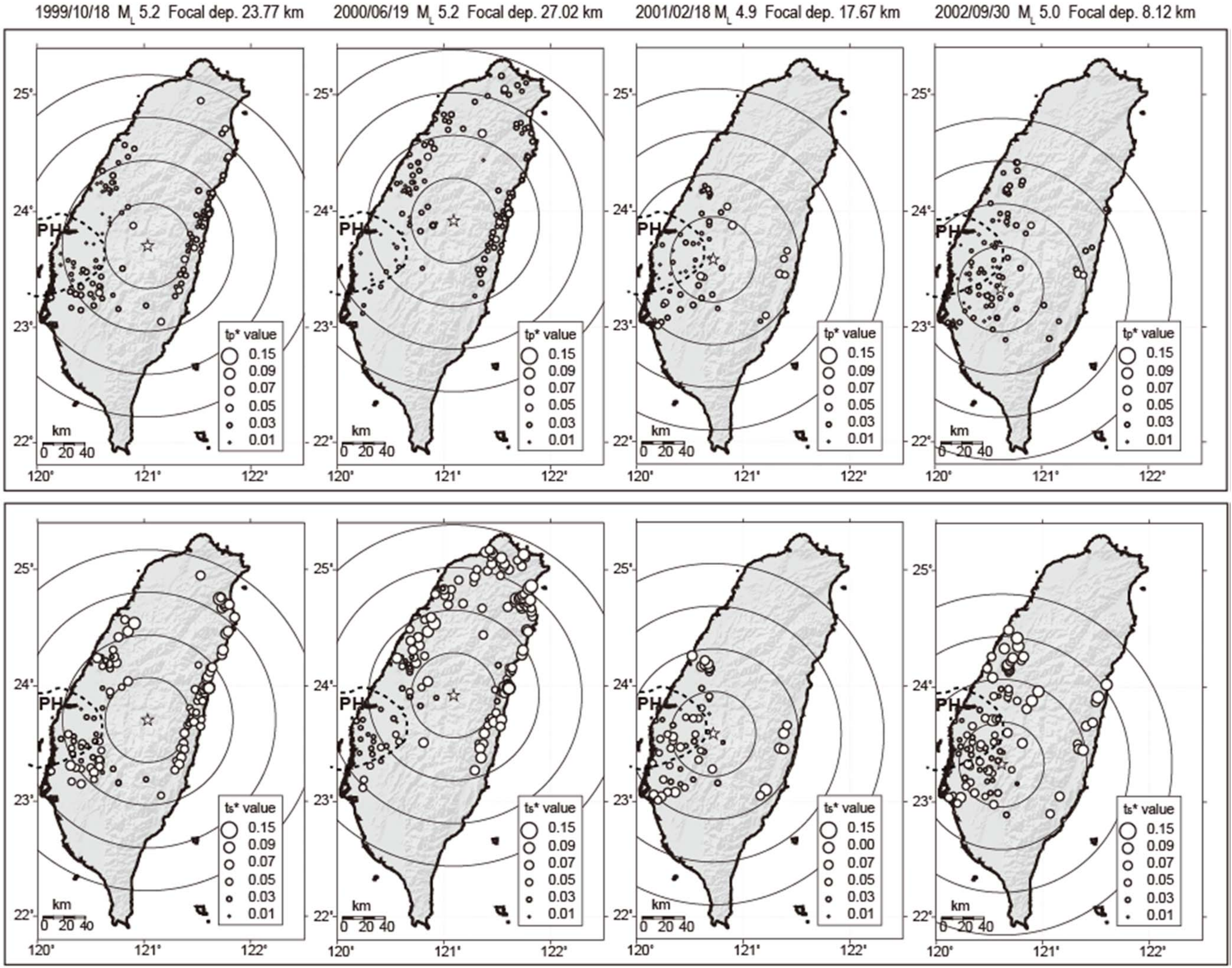

1999/10/18 M_L 5.2 Focal dep. 23.77 km
2000/06/19 M_L 5.2 Focal dep. 27.02 km
2001/02/18 M_L 4.9 Focal dep. 17.67 km
2002/09/30 M_L 5.0 Focal dep. 8.12 km
PH
km
0 20 40
tp* value
0.15
0.09
0.07
0.05
0.03
0.01
ts* value
0.15
0.09
0.00
0.07
0.05
0.03
0.01
25°
24°
23°
22°
120°
121°
122°

Model grid

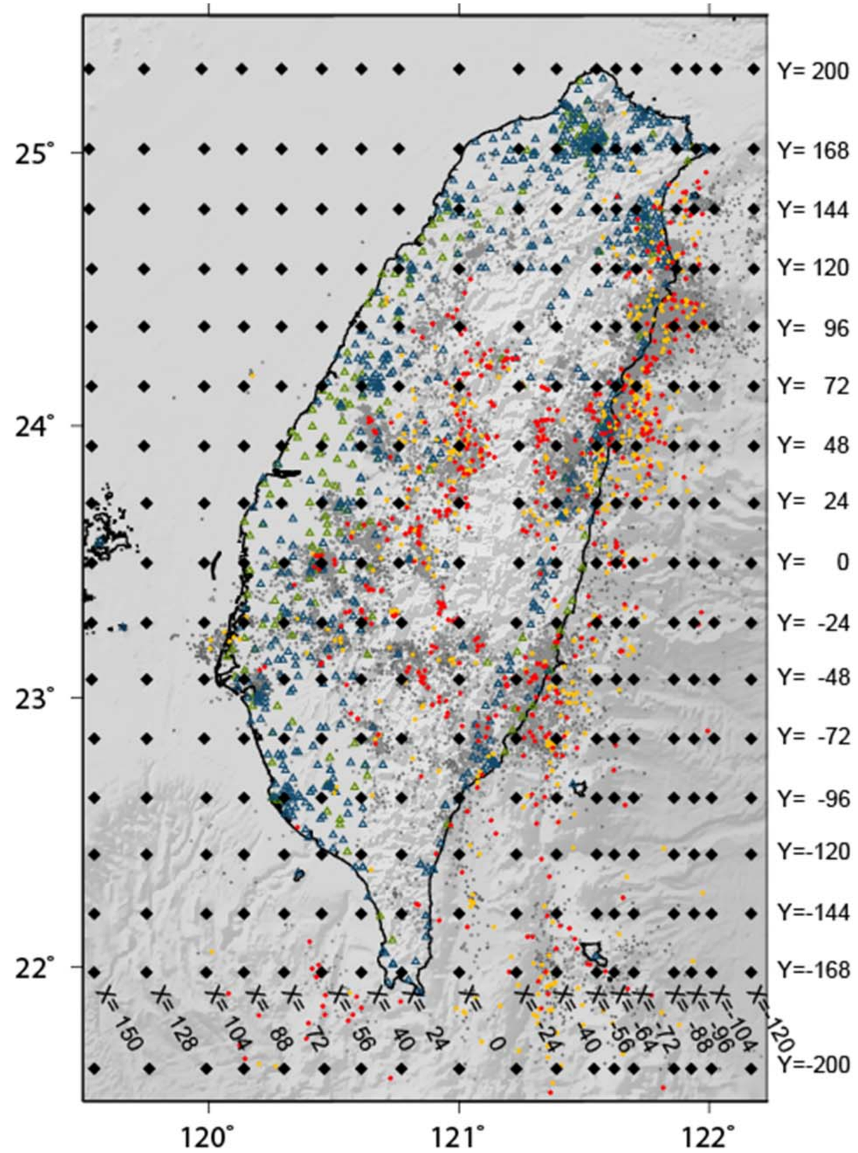

Initial Qp, Qs model

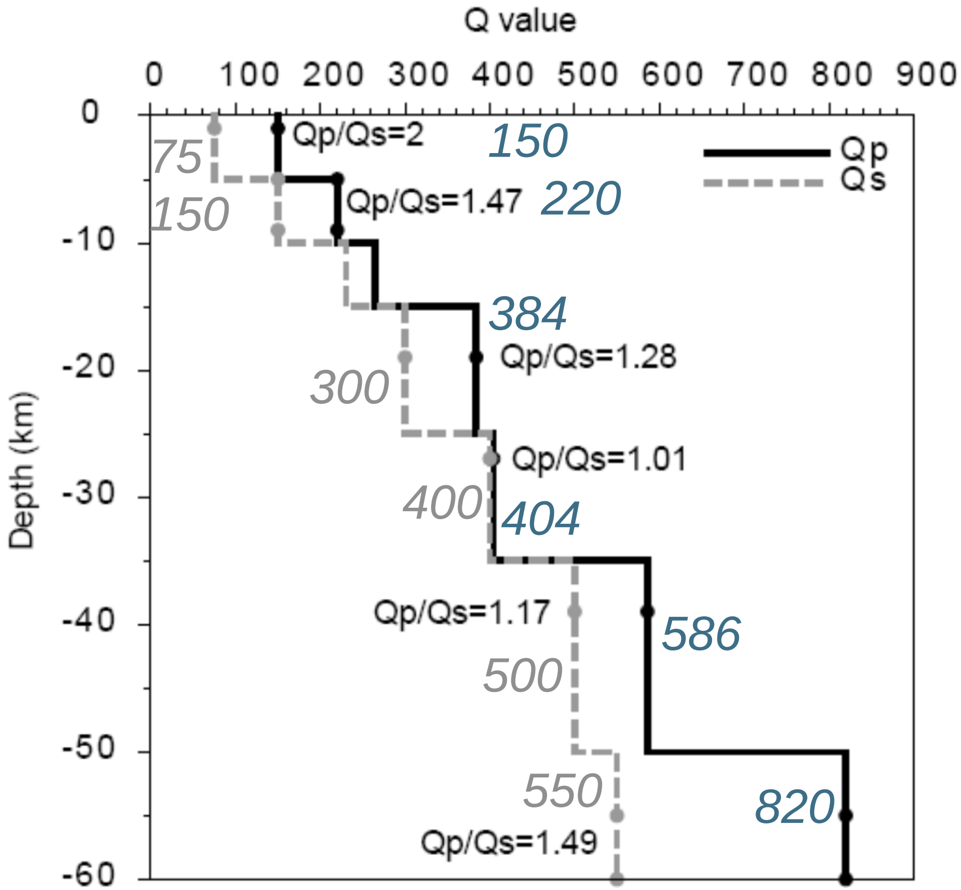

(Chen et al 1996; Chen 1998)

- ***Vp & Vs models***

(Kim et al. 2005)

Spread function

$$M^{est} = RM^{true}$$

$$\begin{bmatrix} m_1 \\ m_2 \\ \vdots \\ m_j \end{bmatrix} = \begin{bmatrix} r_{11} & \cdots & r_{1k} \\ \vdots & \ddots & \vdots \\ r_{j1} & \cdots & r_{jk} \end{bmatrix} \begin{bmatrix} m_1' \\ m_2' \\ \vdots \\ m_j' \end{bmatrix}$$

resolution matrix

$$if \;\; M^{est} = M^{true}$$

$$then \quad r_{jk}=0, j=k$$

$$r_{jk}\neq 0, j\neq k$$

$$R = \begin{bmatrix} 1 & 0 & \cdots & 0 \\ 0 & 1 & 0 & \vdots \\ \vdots & 0 & \ddots & 0 \\ 0 & \cdots & 0 & 1 \end{bmatrix}$$

$$S_j = \log\left[|s_j|^{-1} \sum_{k=1}^{N} \left(\frac{s_{kj}}{|s_j|}\right)^2 \right] D_{jk}$$

Michelinin and McEvilly (1991)

$$j \left\{ \overbrace{\begin{bmatrix} s_1 & s_{21} & . & . & s_{k1} \\ 0 & s_2 & 0 & 0 & 0 \\ . & . & . & . & . \\ . & . & . & . & . \\ s_{1j} & 0 & 0 & 0 & s_j \end{bmatrix}}^{k} \right.$$

D_{jk}

- ***larger S_j , more smearing***

Qp, Qs Tomography images

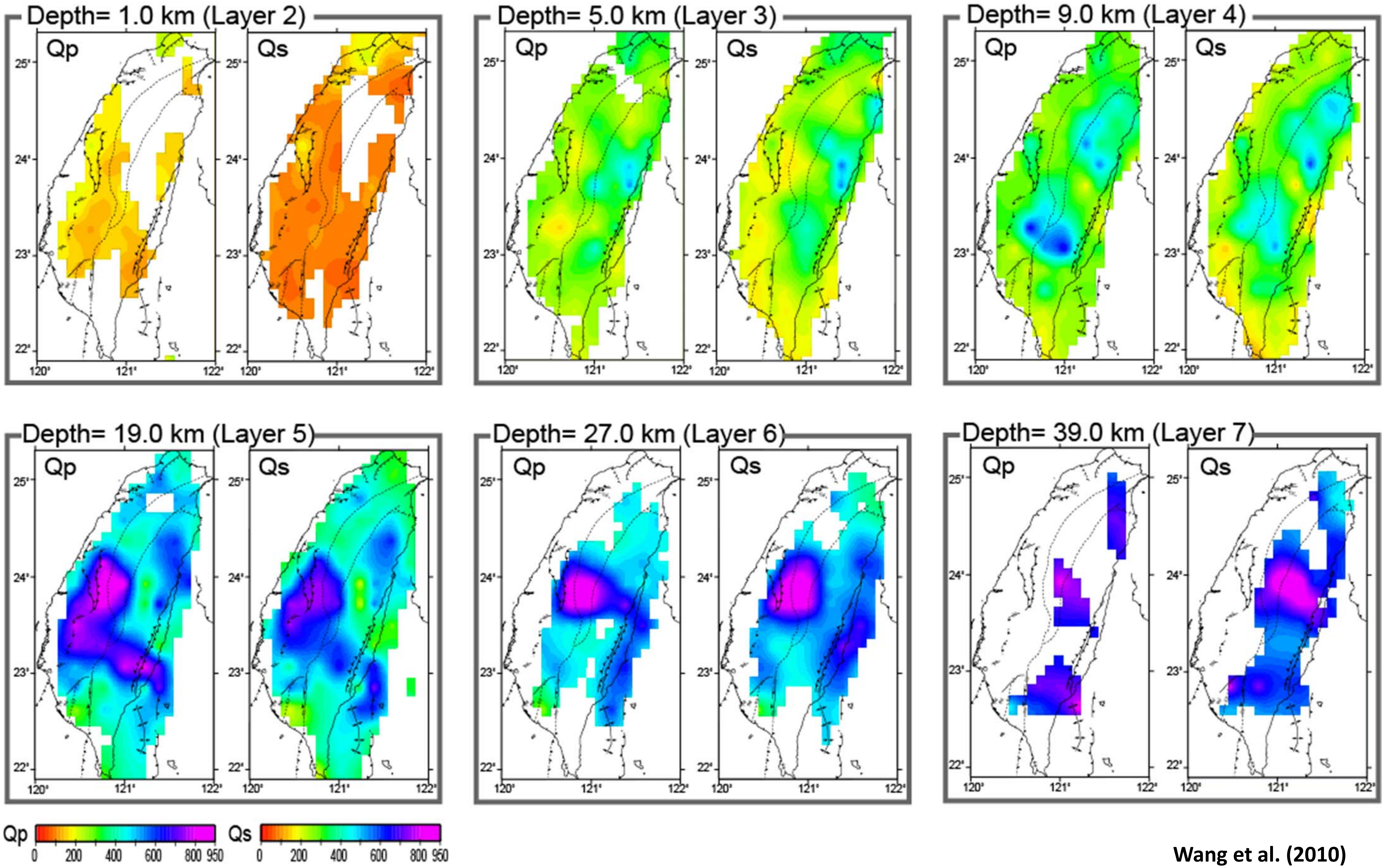

Wang et al. (2010)

Chelungpu Fault

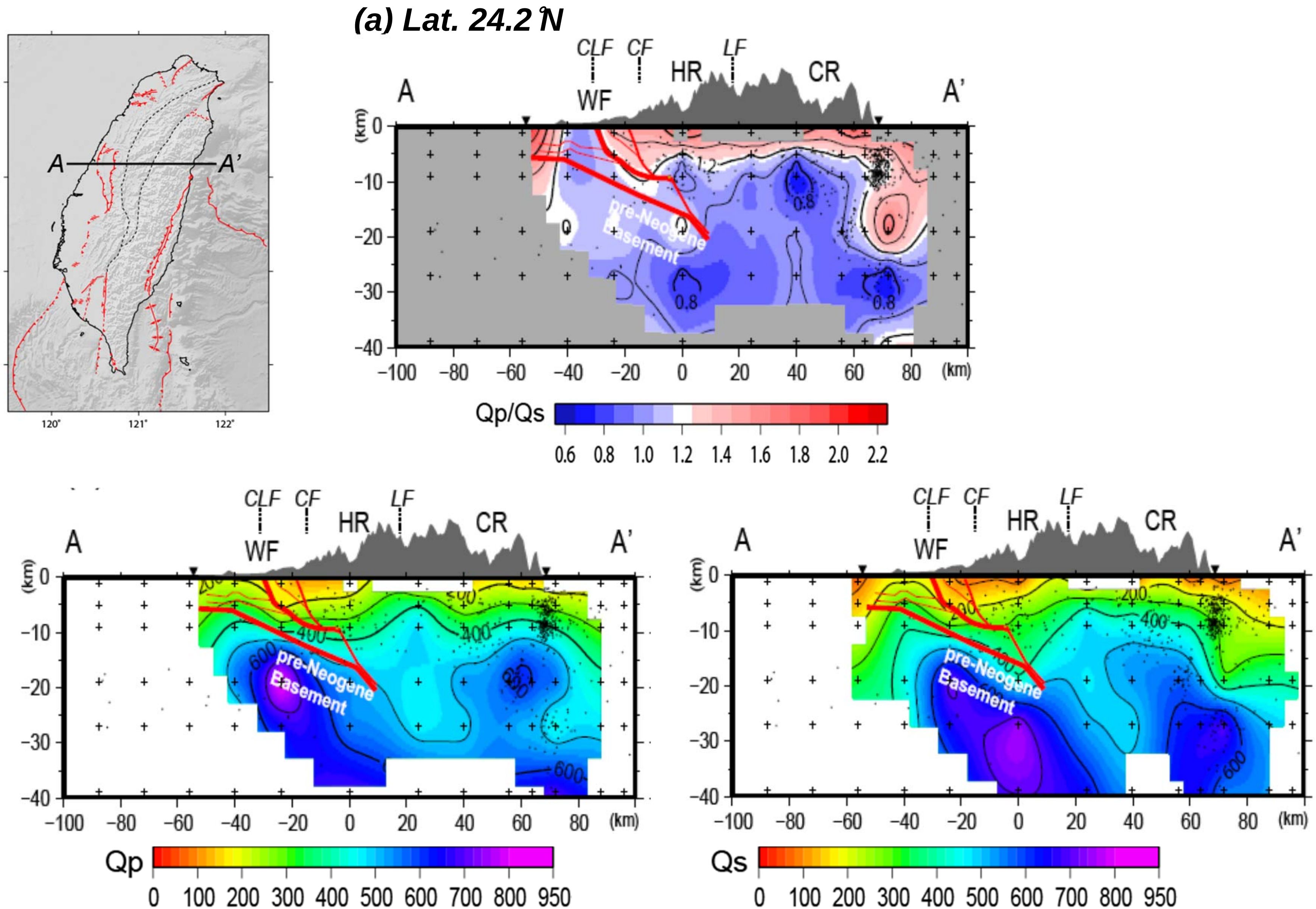

Wang et al. (2010)

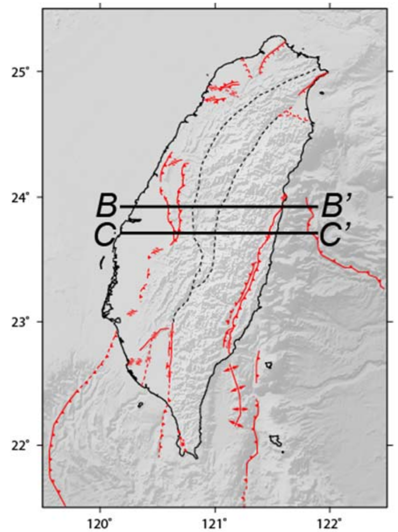

Peikang High \ Central Range

Peikang High

✓High Qp, Qs

Central Range

✓Aseismic Zone

✓High Temperature

(Ma et al. 1996; Lin 2000;

Simoes et al. 2007; Yamato et al. 2008**)**

✓Ductile ***(Kim et al. 2005)***

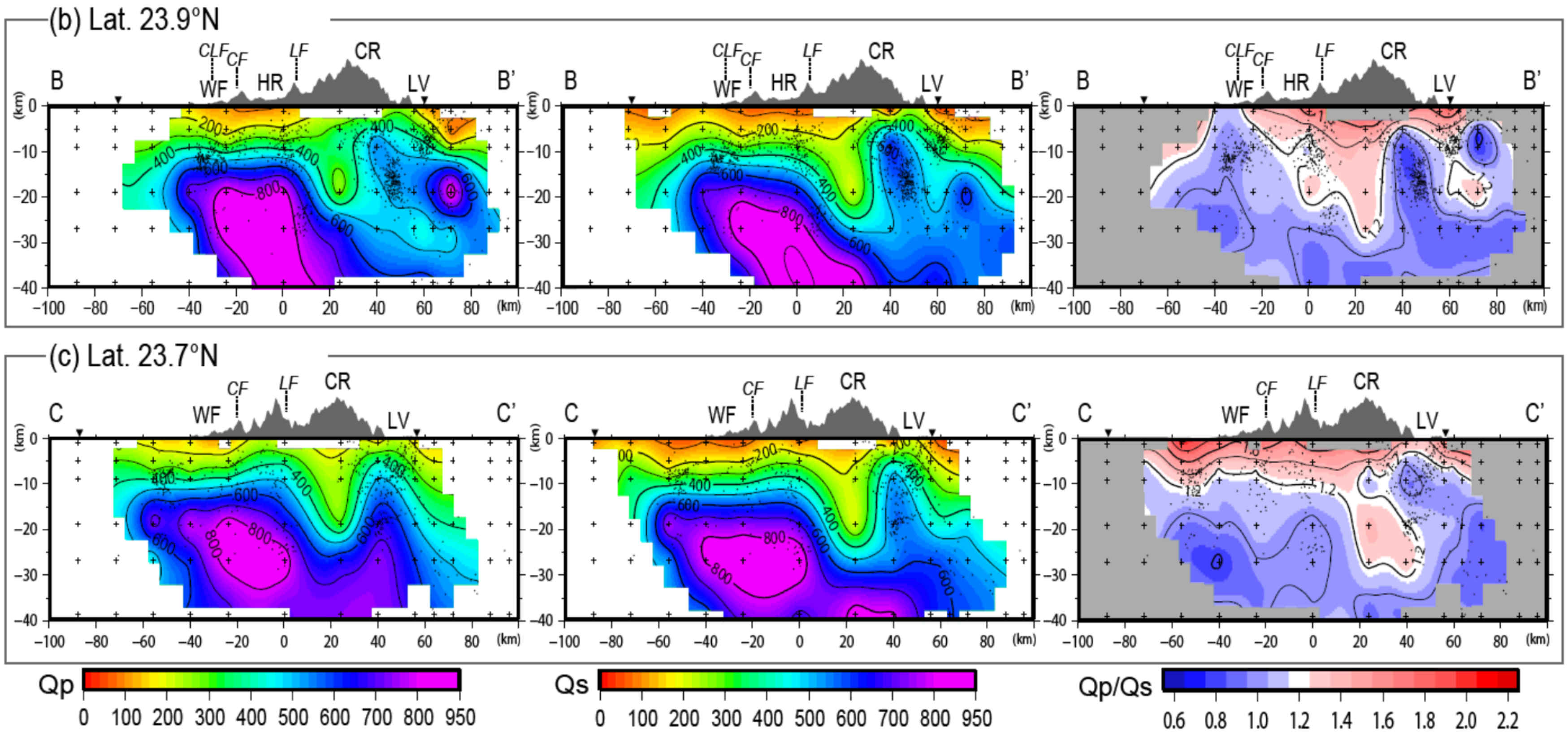

Pingtung Plain

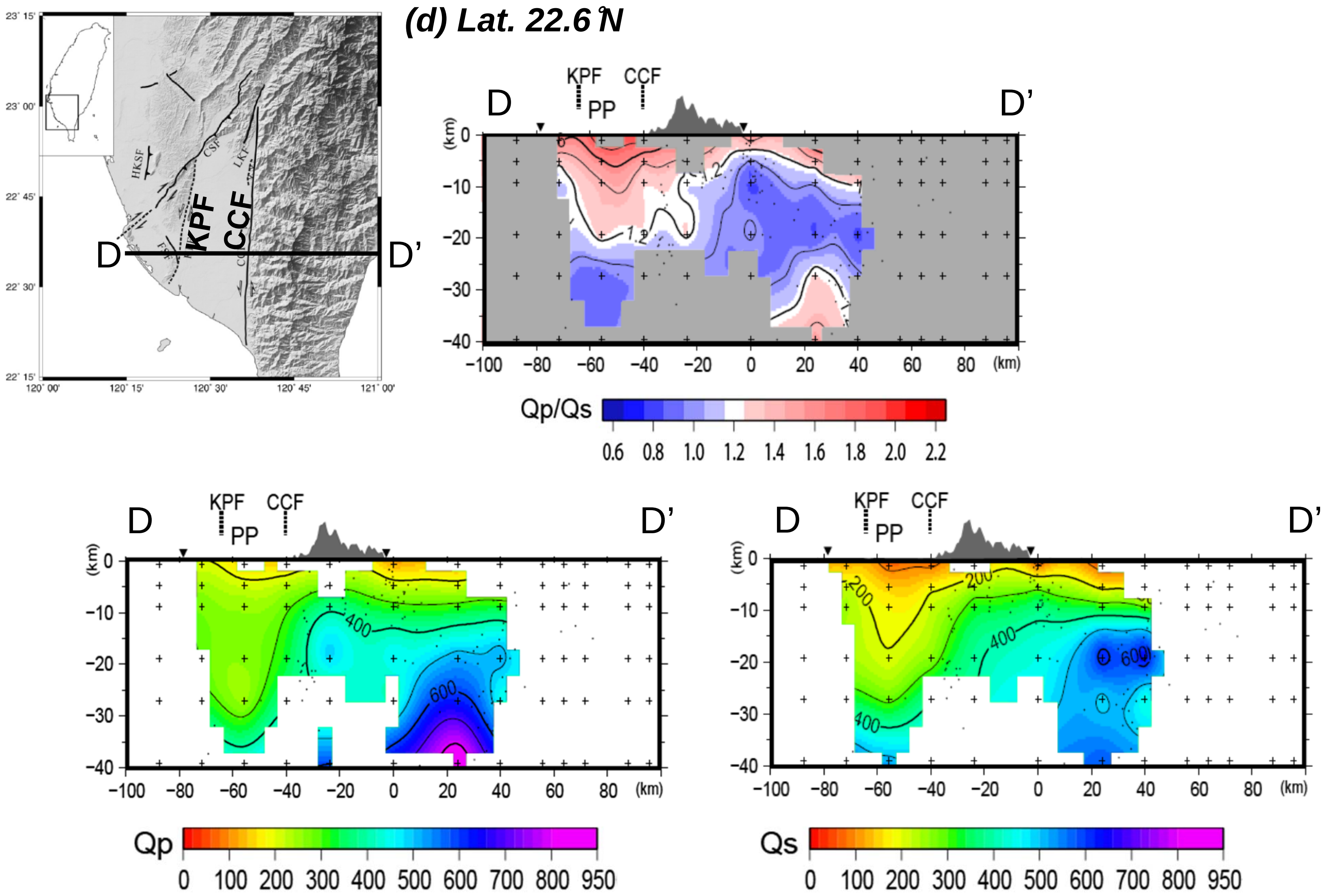

- High Qp/Qs, low Qp, Qs are associated with the unconsolidated coastal and estuarine sediments within fully fluid-saturated property of Pingtung Plain.

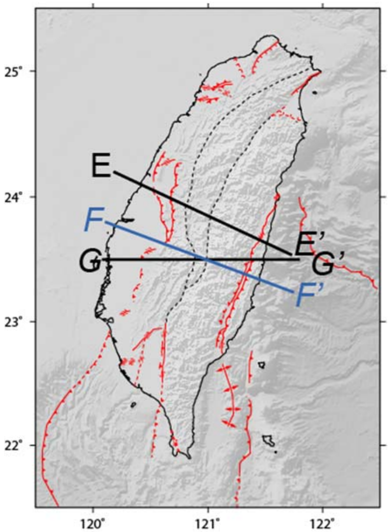

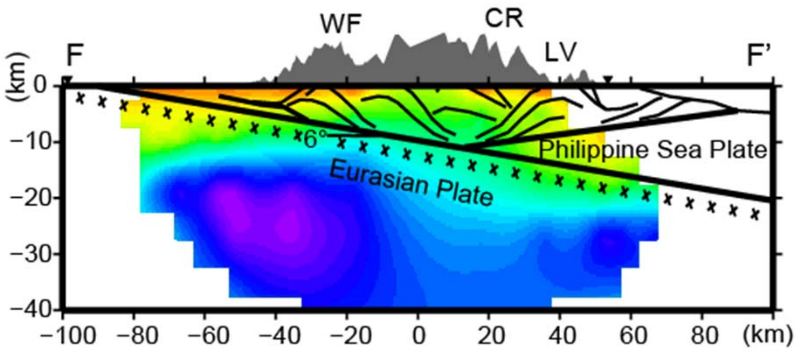

●Thin-skinned model

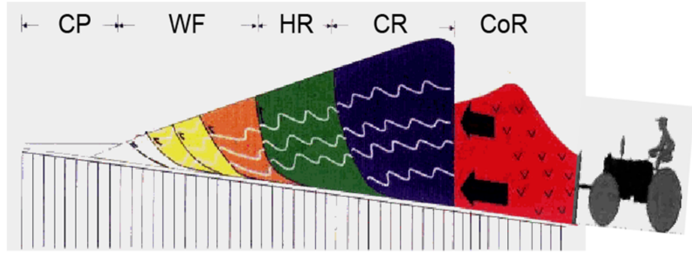

(Suppe 1981)

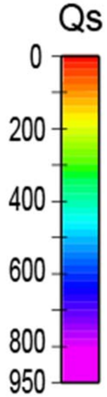

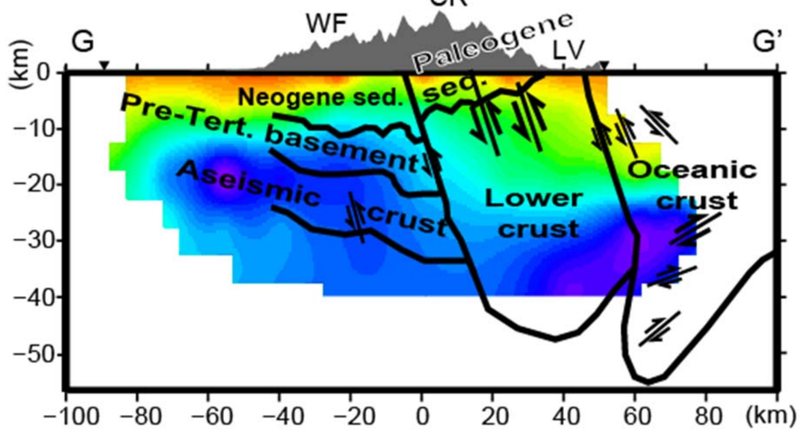

●Lithospheric collision model

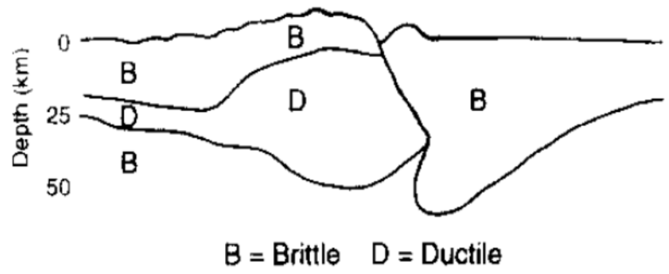

(Wu et al. 1997)

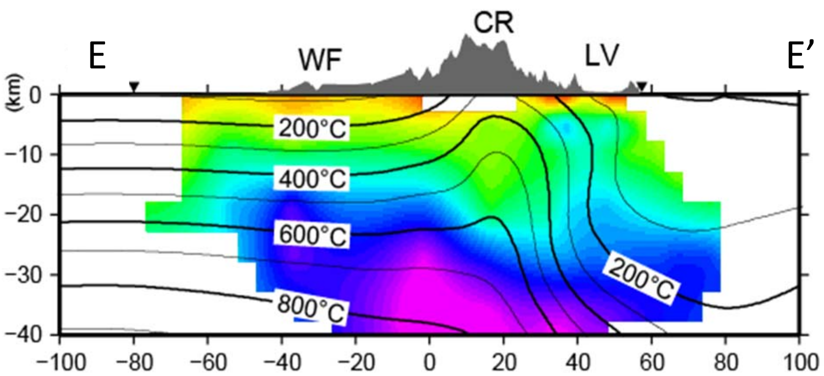

●Thermo-mechanical model

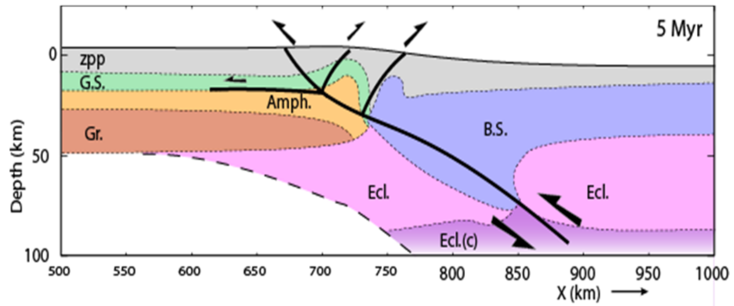

(Yamato et al. 2009)

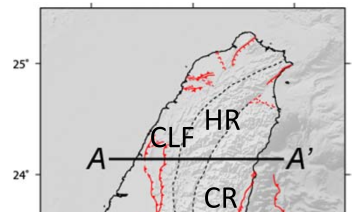

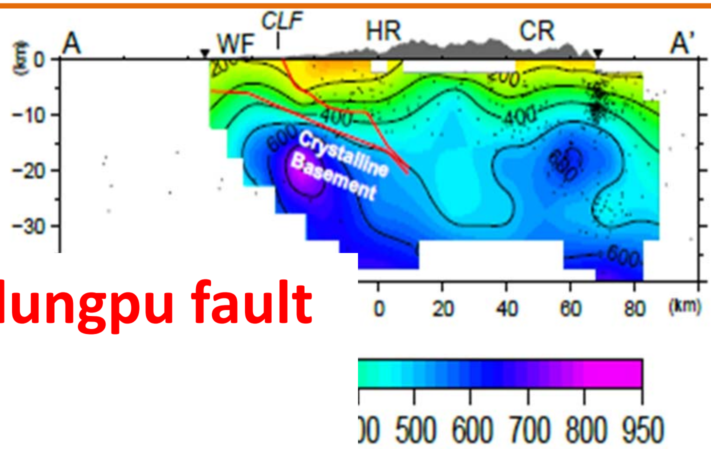

How is the Q within the ruptured Chelungpu fault zone?

Is the low Q related to the occurrence of Chi-Chi earthquake? Yes!

Q f

Su

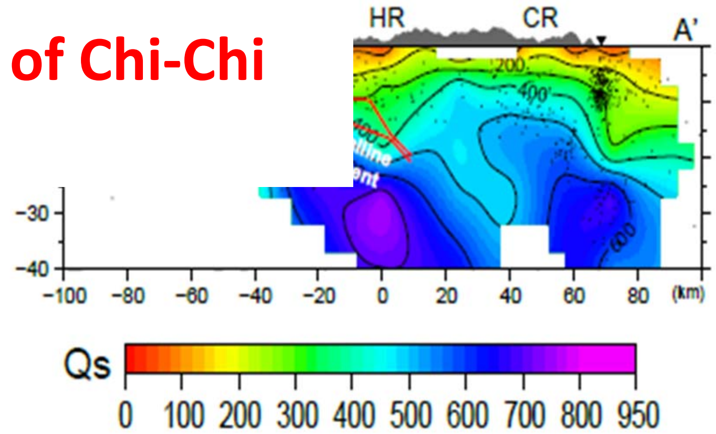

(Sanders *et al.*, 1995)

Rock State Change	Seismic Parameter Change			
	Qs	*Qp*	*Qp/Qs*	*Vp/Vs*
Increase temperature	smaller	smaller	larger	larger
Partial melt	much smaller	smaller	much larger	much larger
Increase fracture abundance (Increase fluid)	smaller	smaller	larger	larger
Add gas or supercritical	larger	much smaller	much smaller	smaller

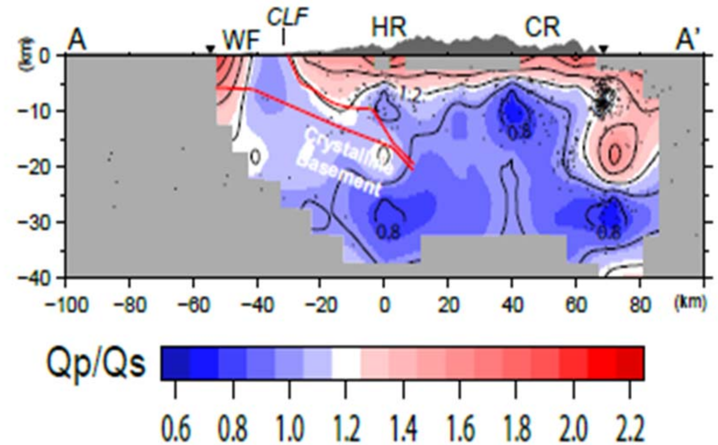

The attenuation features within the Chelungpu fault zone

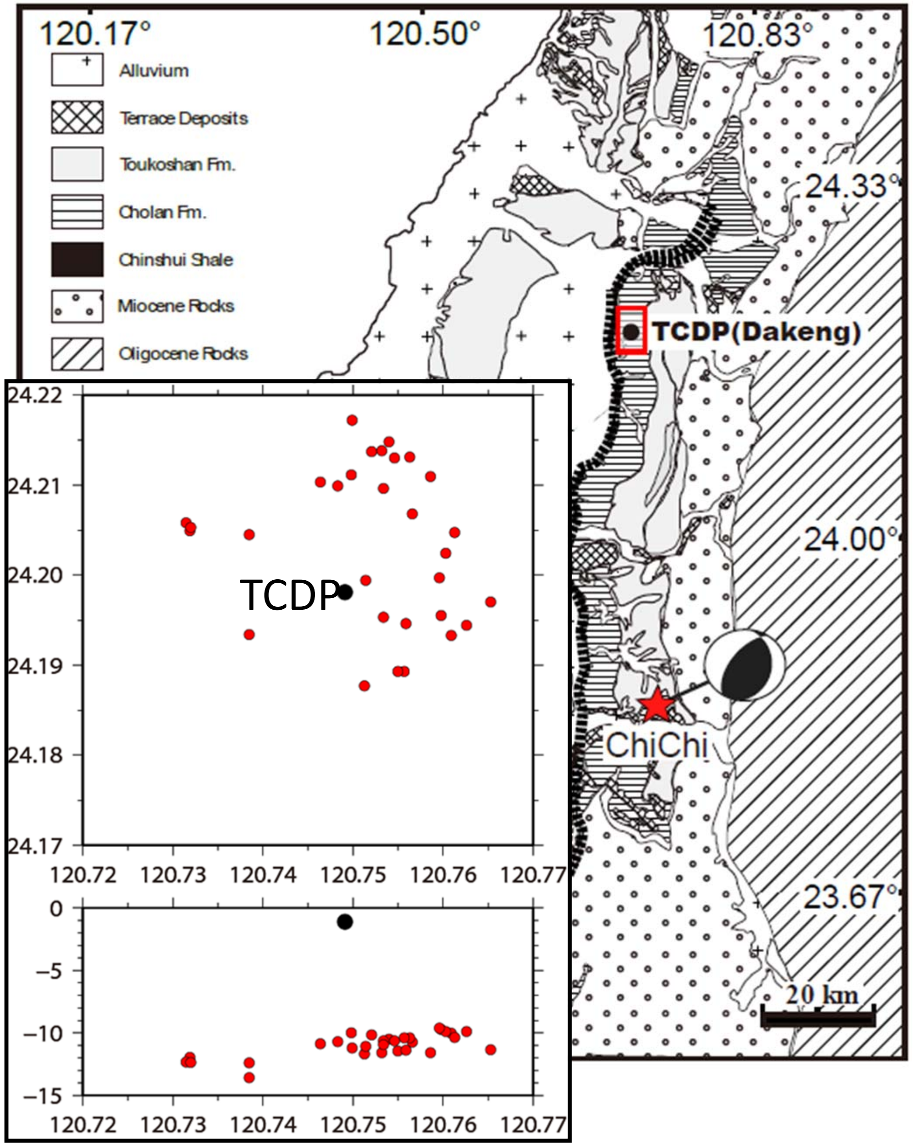

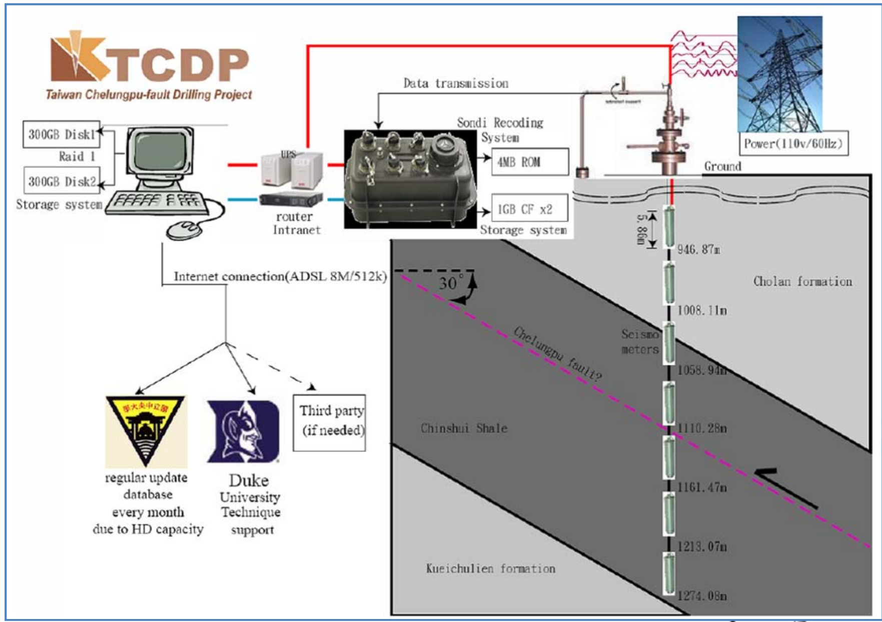

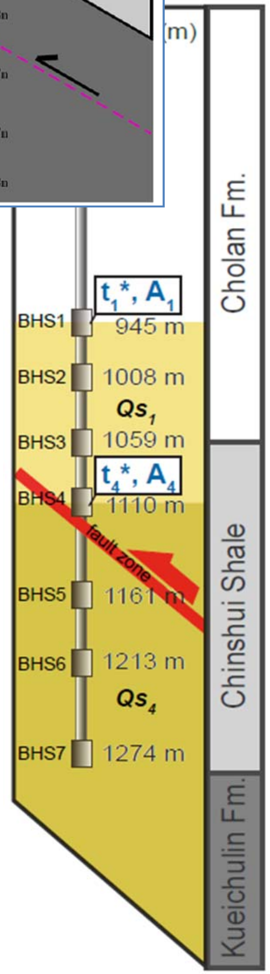

Spectral Ratio Method:

$$A_1(f) = 2\pi f \Omega_0 \frac{fc^2}{f^2 + fc^2} e^{-\pi f t_1^*}$$

$$A_4(f) = 2\pi f \Omega_0 \frac{fc^2}{f^2 + fc^2} e^{-\pi f t_4^*}$$

$$\ln R(f) = \ln(A) - \pi f (t_1^* - t_4^*)$$

$$t_1^* - t_4^* = \frac{ds_{1.11-0.945}}{Qs_1 Vs_1} = \frac{t_1 - t_4}{Qs_1}$$

2006/11-2007/4

Incident angle < 10°

Total 26 events with high S/N were used.

Mw 0.28-1.5

Wang et al. (2012)

P-wave

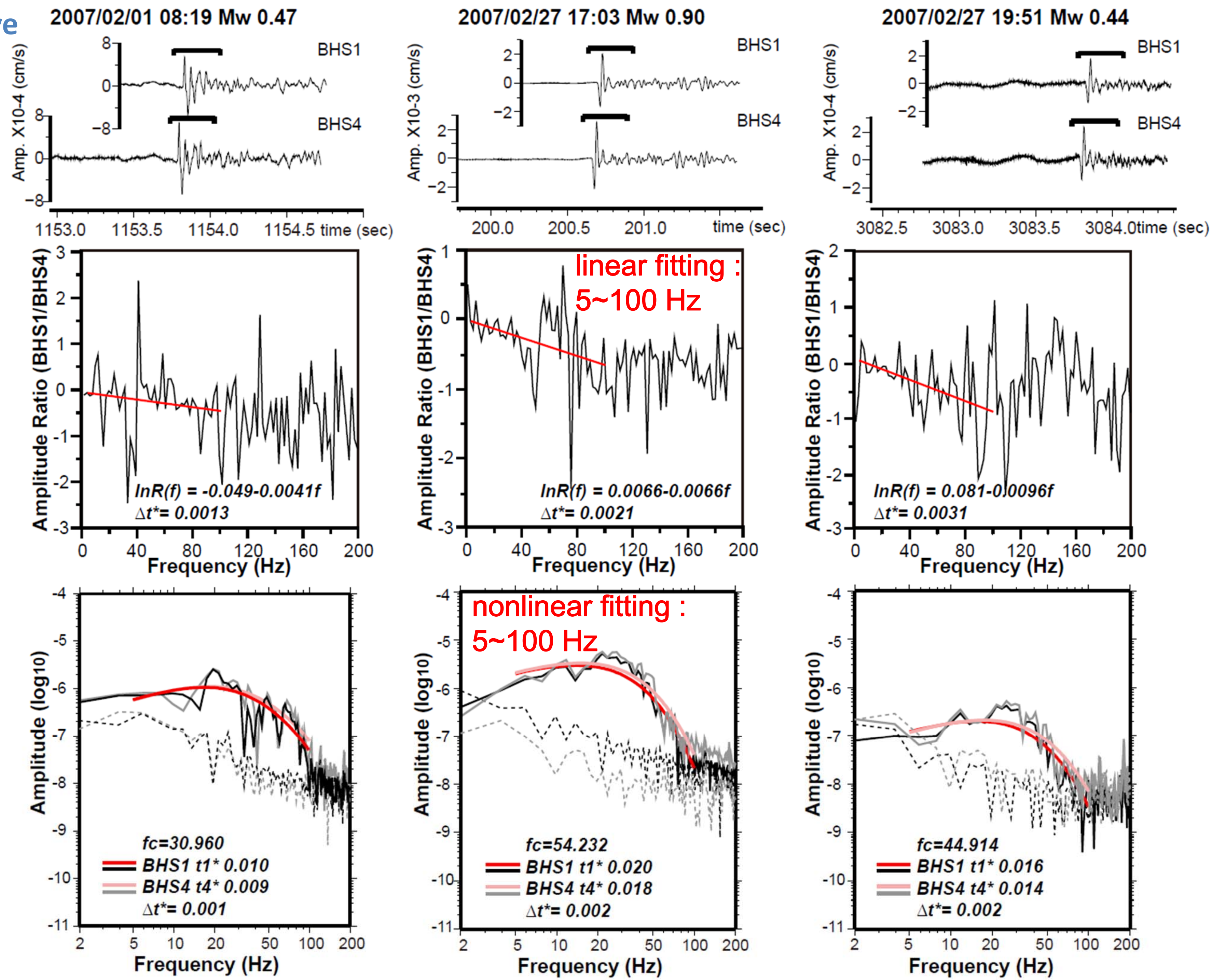

2007/02/01 08:19 Mw 0.47
2007/02/27 17:03 Mw 0.90
2007/02/27 19:51 Mw 0.44
BHS1
BHS4
Amp. X10-4 (cm/s)
Amp. X10-3 (cm/s)
time (sec)
Amplitude Ratio (BHS1/BHS4)
Frequency (Hz)
linear fitting : 5~100 Hz
lnR(f) = -0.049-0.0041f
Δt*= 0.0013
lnR(f) = 0.0066-0.0066f
Δt*= 0.0021
lnR(f) = 0.081-0.0096f
Δt*= 0.0031
nonlinear fitting : 5~100 Hz
Amplitude (log10)
fc=30.960
BHS1 t1* 0.010
BHS4 t4* 0.009
Δt*= 0.001
fc=54.232
BHS1 t1* 0.020
BHS4 t4* 0.018
Δt*= 0.002
fc=44.914
BHS1 t1* 0.016
BHS4 t4* 0.014
Δt*= 0.002

S-wave

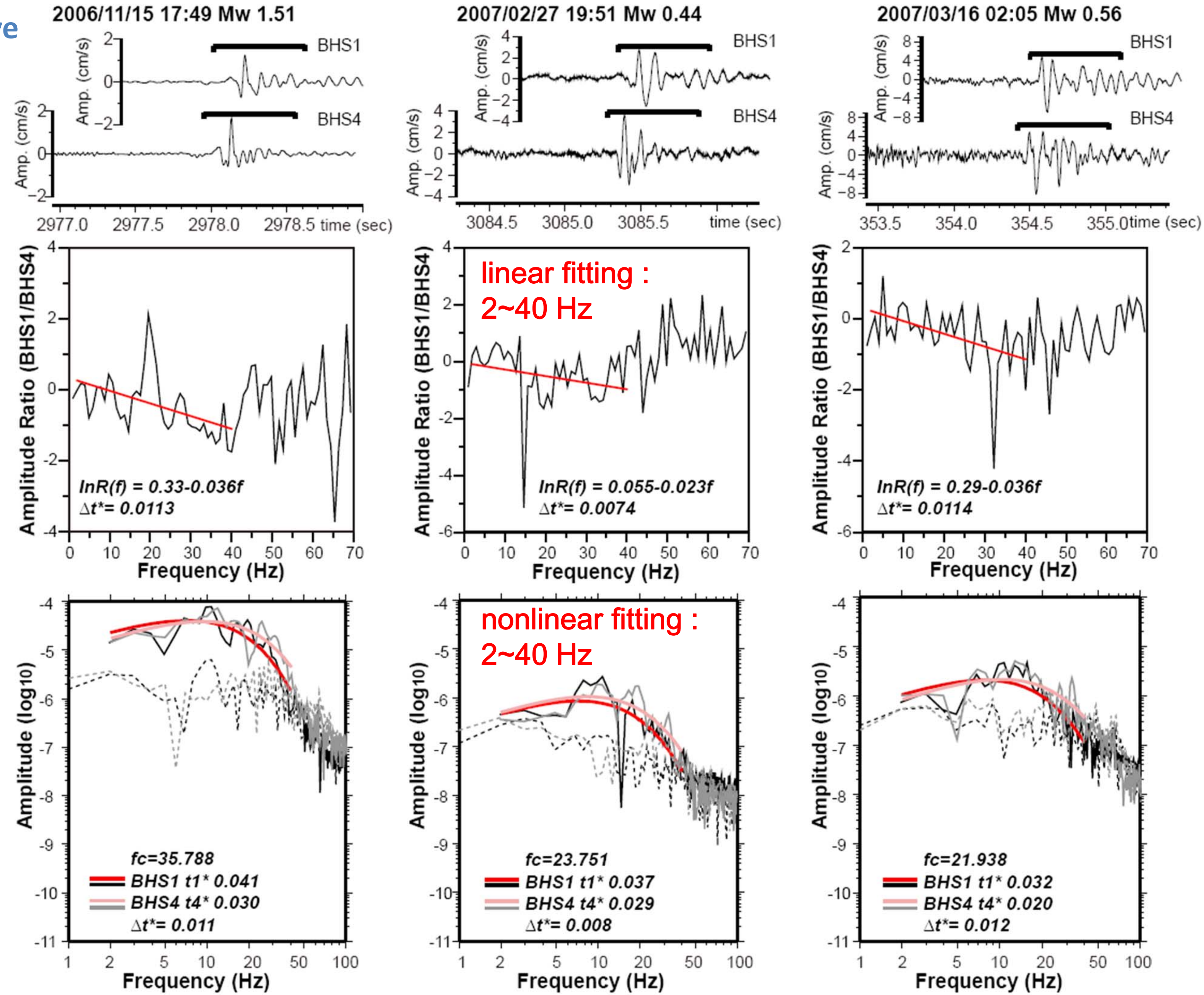

2006/11/15 17:49 Mw 1.51
2007/02/27 19:51 Mw 0.44
2007/03/16 02:05 Mw 0.56
BHS1
BHS4
Amp. (cm/s)
time (sec)
Amplitude Ratio (BHS1/BHS4)
Frequency (Hz)
linear fitting :
2~40 Hz
lnR(f) = 0.33-0.036f
Δt*= 0.0113
lnR(f) = 0.055-0.023f
Δt*= 0.0074
lnR(f) = 0.29-0.036f
Δt*= 0.0114
nonlinear fitting :
2~40 Hz
Amplitude (log10)
fc=35.788
BHS1 t1* 0.041
BHS4 t4* 0.030
Δt*= 0.011
fc=23.751
BHS1 t1* 0.037
BHS4 t4* 0.029
Δt*= 0.008
fc=21.938
BHS1 t1* 0.032
BHS4 t4* 0.020
Δt*= 0.012

The estimation of t*

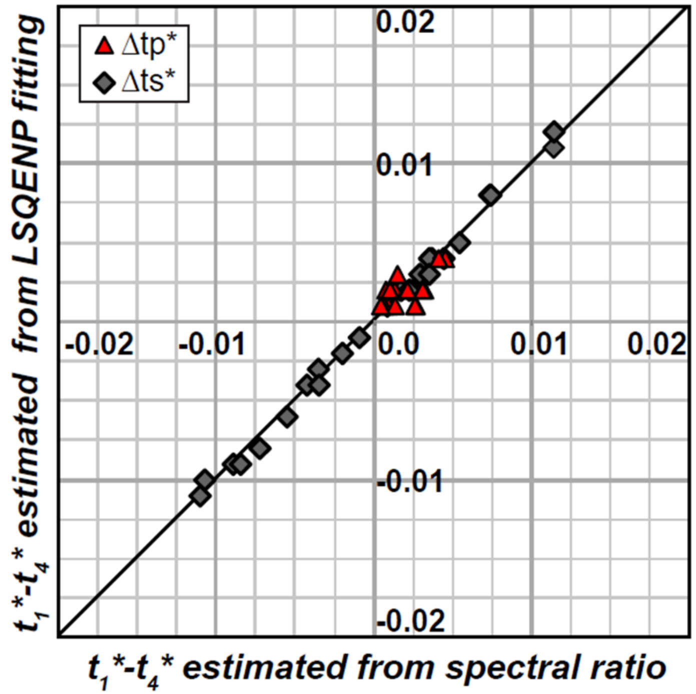

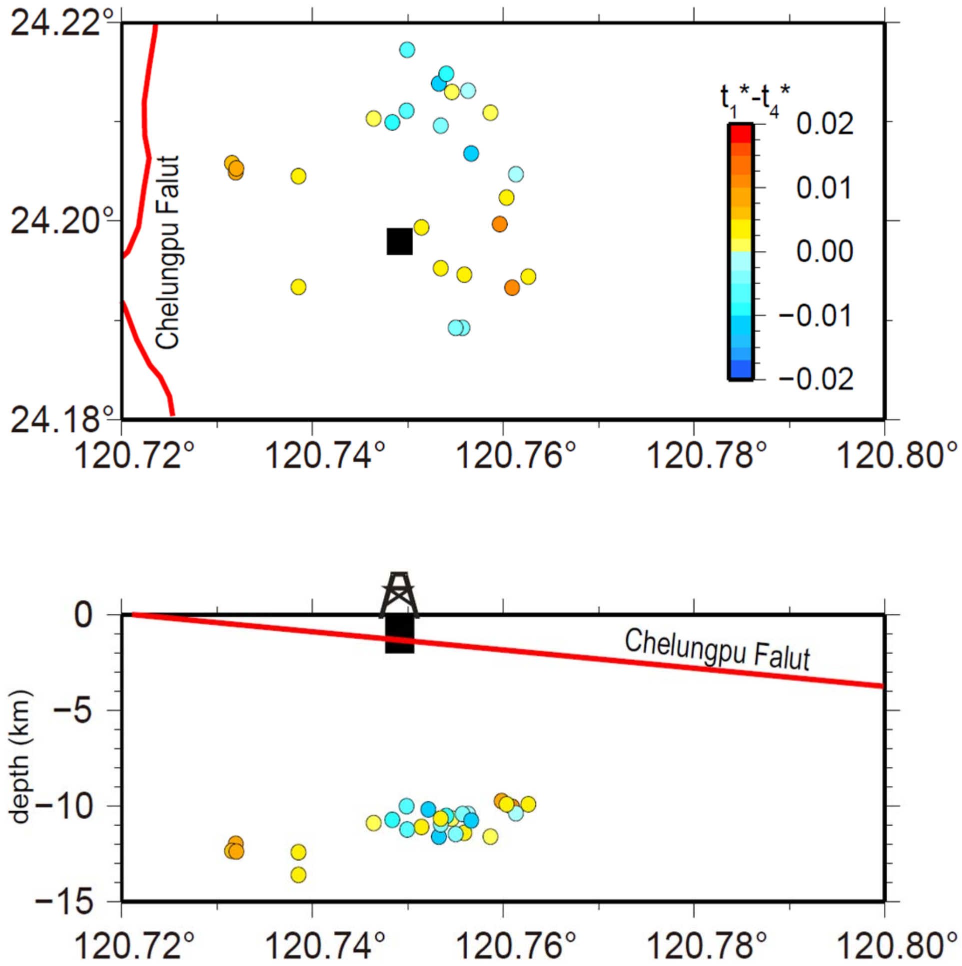

$t_1^*-t_4^* < 0$

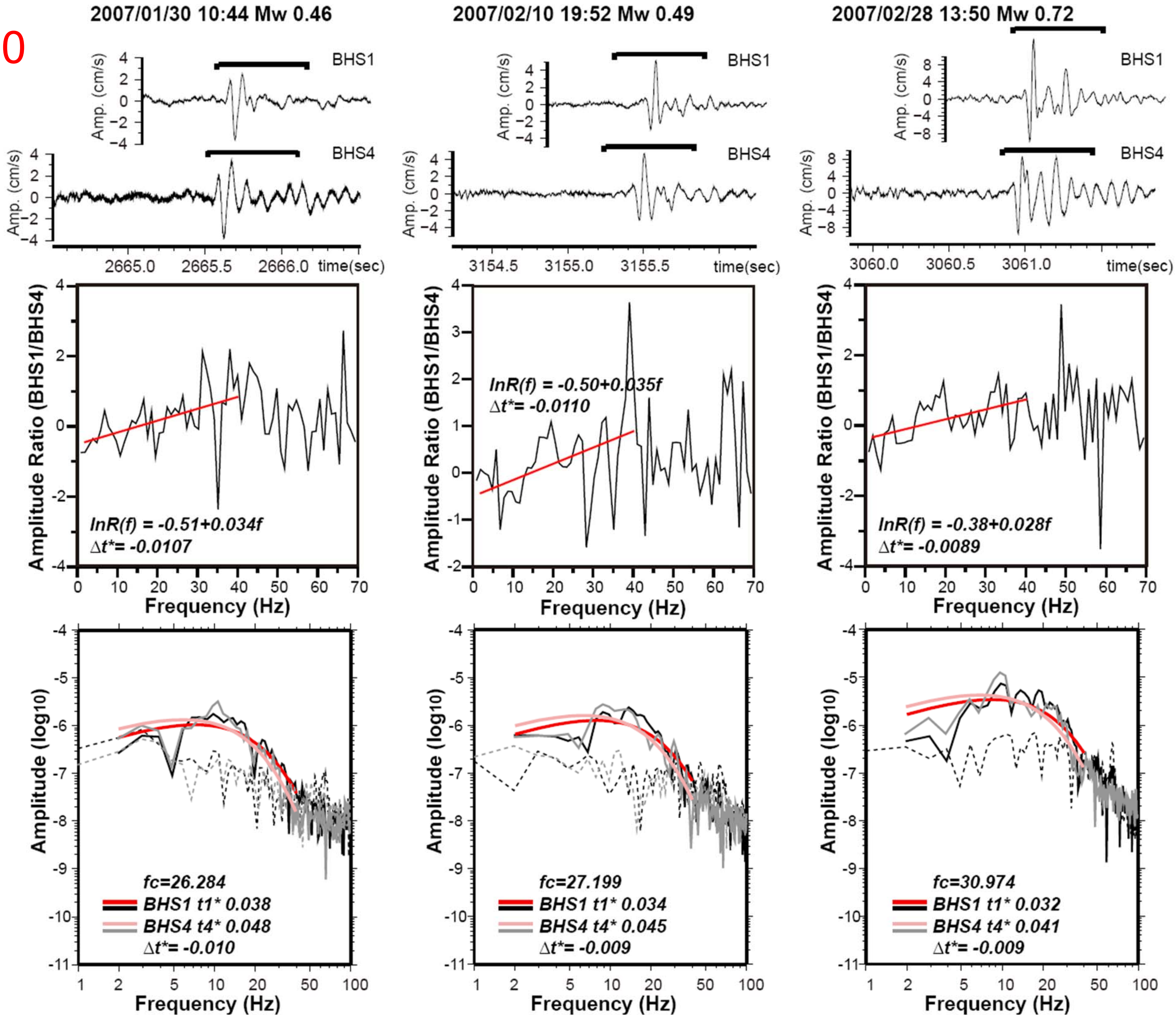

2007/01/30 10:44 Mw 0.46
2007/02/10 19:52 Mw 0.49
2007/02/28 13:50 Mw 0.72
BHS1
BHS4
Amp. (cm/s)
time(sec)
Amplitude Ratio (BHS1/BHS4)
Frequency (Hz)
lnR(f) = -0.51+0.034f
Δt*= -0.0107
lnR(f) = -0.50+0.035f
Δt*= -0.0110
lnR(f) = -0.38+0.028f
Δt*= -0.0089
Amplitude (log10)
fc=26.284
BHS1 t1* 0.038
BHS4 t4* 0.048
Δt*= -0.010
fc=27.199
BHS1 t1* 0.034
BHS4 t4* 0.045
Δt*= -0.009
fc=30.974
BHS1 t1* 0.032
BHS4 t4* 0.041
Δt*= -0.009

A selection of near-surface attenuation results in borehole (≥100 m) studies in California.

Location	Depth Range (m)	Q_P	Q_S	Rock Type	Authors
Oroville	0–475	—	9	ophiolite	Malin *et al.* (1988)
Oroville	375–475	—	11	ophiolite	Malin *et al.* (1988)
Anza	0–150	6.5	9	granite	Aster and Shearer (1991)
Anza	150–300	27	26	granite	Aster and Shearer (1991)
Garner Valley	0–220	—	12	soil, weathered granite, and granite	Archuleta *et al.* (1992)
Santa Clara Valley	10–35	—	10	Quaternary alluvium	Gibbs *et al.* (1994)
Santa Clara Valley	40–115	—	15	Quaternary alluvium	Gibbs *et al.* (1994)
Parkfield	0–200	6–11	8–19	Tertiary sediments	Blakeslee and Malin (1991)
Parkfield	0–300	—	10	Tertiary sediments	Jongmans and Malin (1995)
Parkfield	0–1000	—	37	Tertiary sediments	Jongmans and Malin (1995)
Los Angeles basin	0–420	45	—	Pleistocene and Pliocene sediments	Hauksson *et al.* (1987)
Los Angeles basin	420–1500	43	25	Pleistocene and Pliocene sediments	Hauksson *et al.* (1987)
Cajon Pass	**700-1500**	**36±11**	**24 ±6**	**Mesozoic crystalline basement**	**Abercrombie (1997)**

Table 2. *Q* as a Function of Depth Within the Varian Well: From This Study and *Jongmans and Malin* [1995]

Depth Interval, m	Q_P	Q_S	Error	Q_S From *J&M*
0–298	~20	~10	-	8 (7-9)
298-572	-	-	-	8 (7.7-9)
298–938	30	31	25	-
572–938	55	-	30	65 (53-94)
(0 & 23.5) – 938	33	18	30	37 (33-45)

(Abercrombie, 2000)

Chelungpu fault:

Qs_1 (945-1110 m): 21-22

Qp_1 : 27-35

Qs_4 (1110-2000 m): 45

Qp_4 : 85

Wang et al. (2012)

→ *The consistency implies that the existence of fluid, fracture and crack may dominate the attenuation feature of the near surface materials around the fault zone rather than the rock type.*

The subsurface attenuation model of Taiwan (depth ~300 m depth)

CWB borehole network

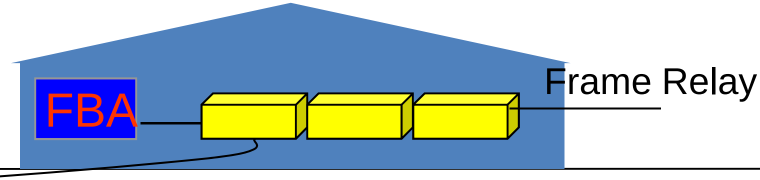

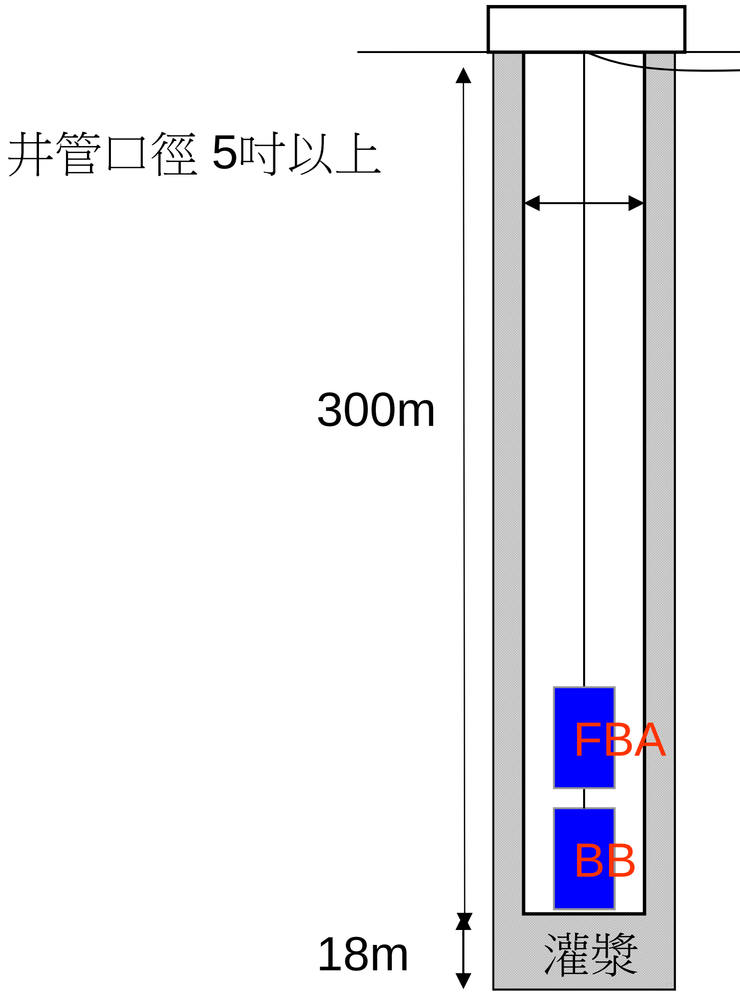

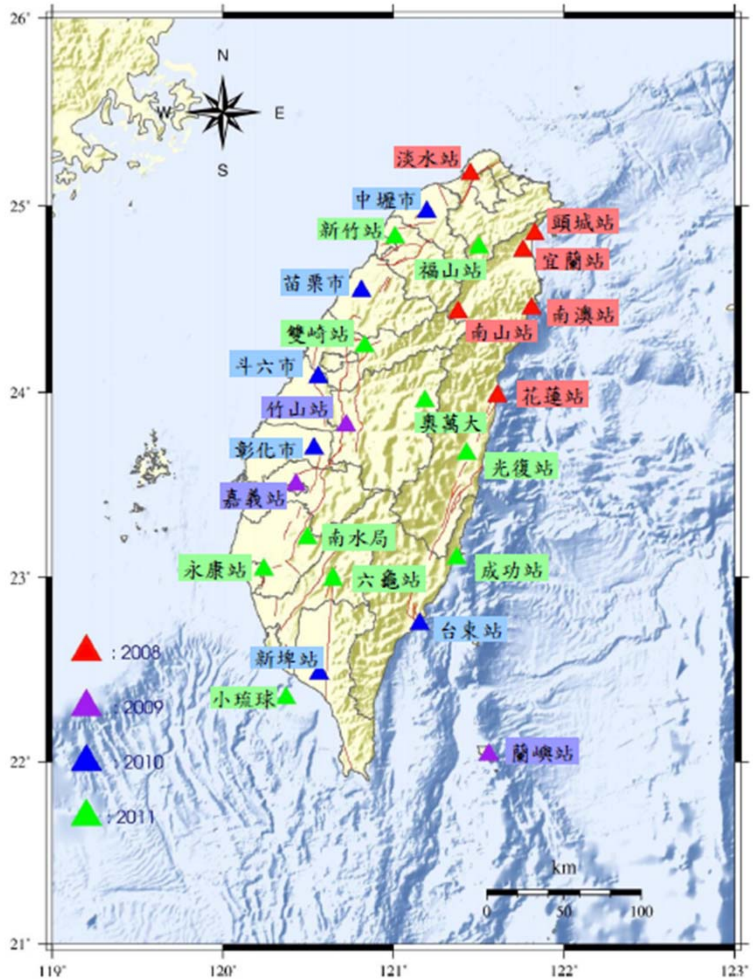

23 stations
until 2012/02

CWB borehole data

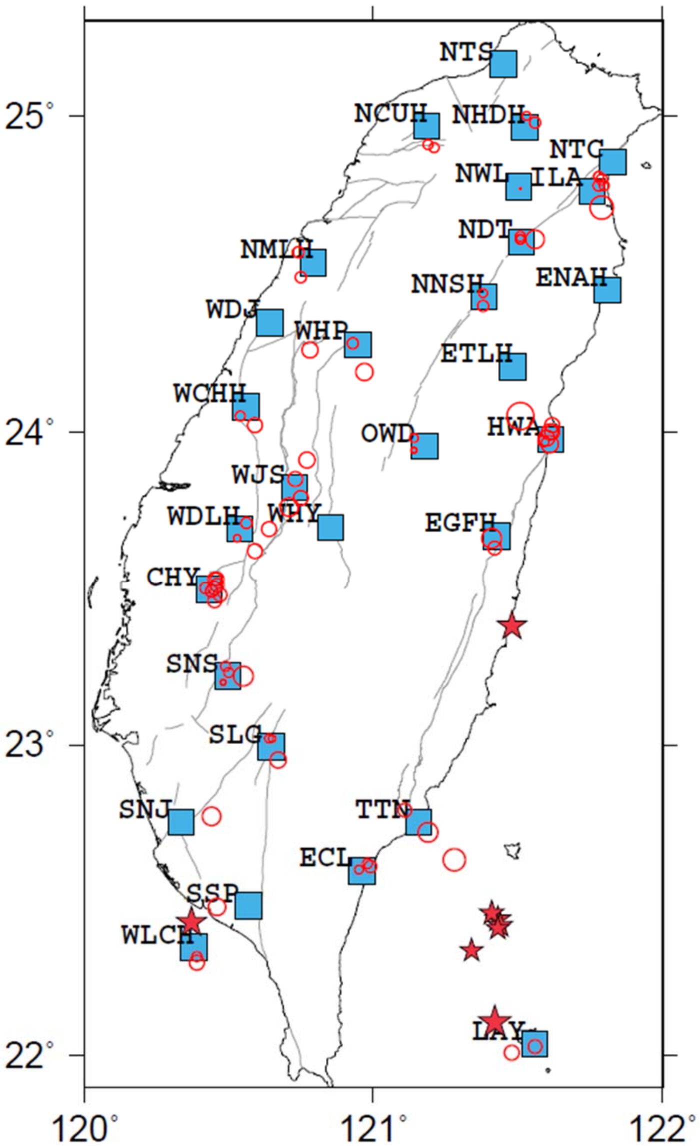

- Data period: 2011/10-2013/05
- high SN ratio and low incidence angle (< 35 deg.)
- **67 events** (ML < 4.5)

- **8 events** (4.0 < ML < 6.0 ; 18 km < Depth < 77 km)

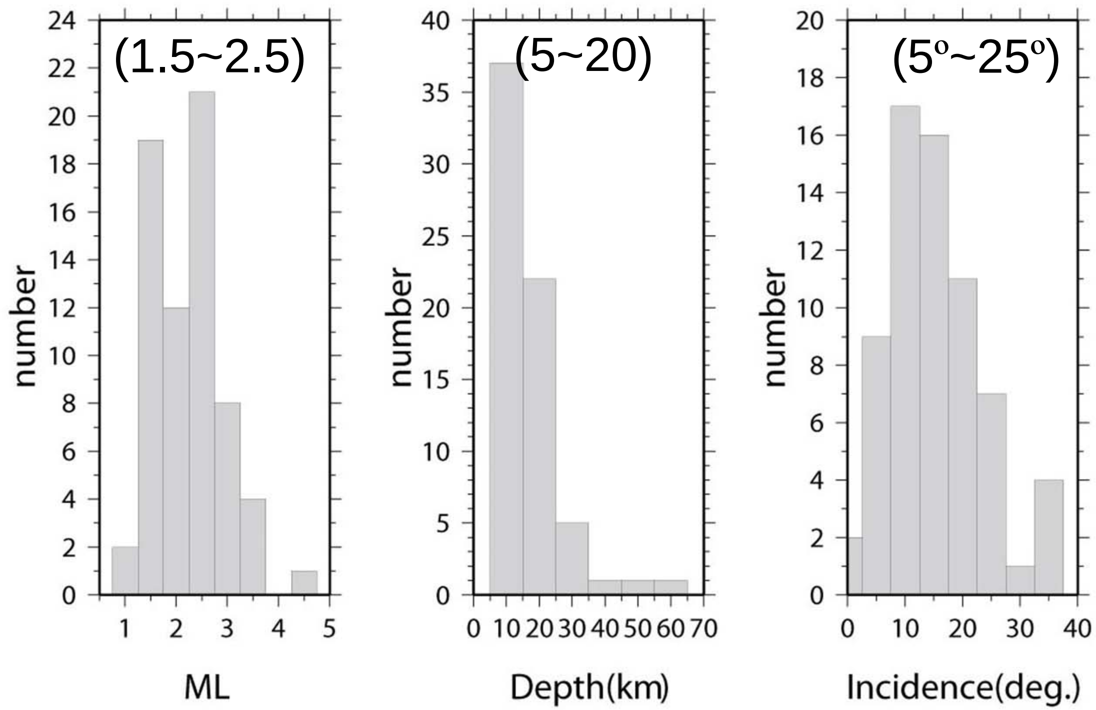

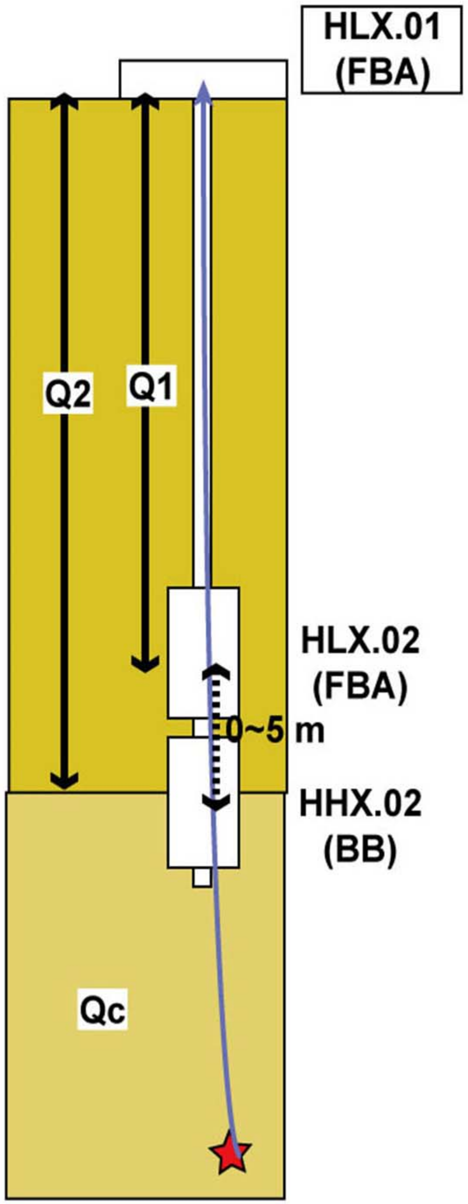
HLX.01
(FBA)
Q2
Q1
HLX.02
(FBA)
0~5 m
HHX.02
(BB)
Qc

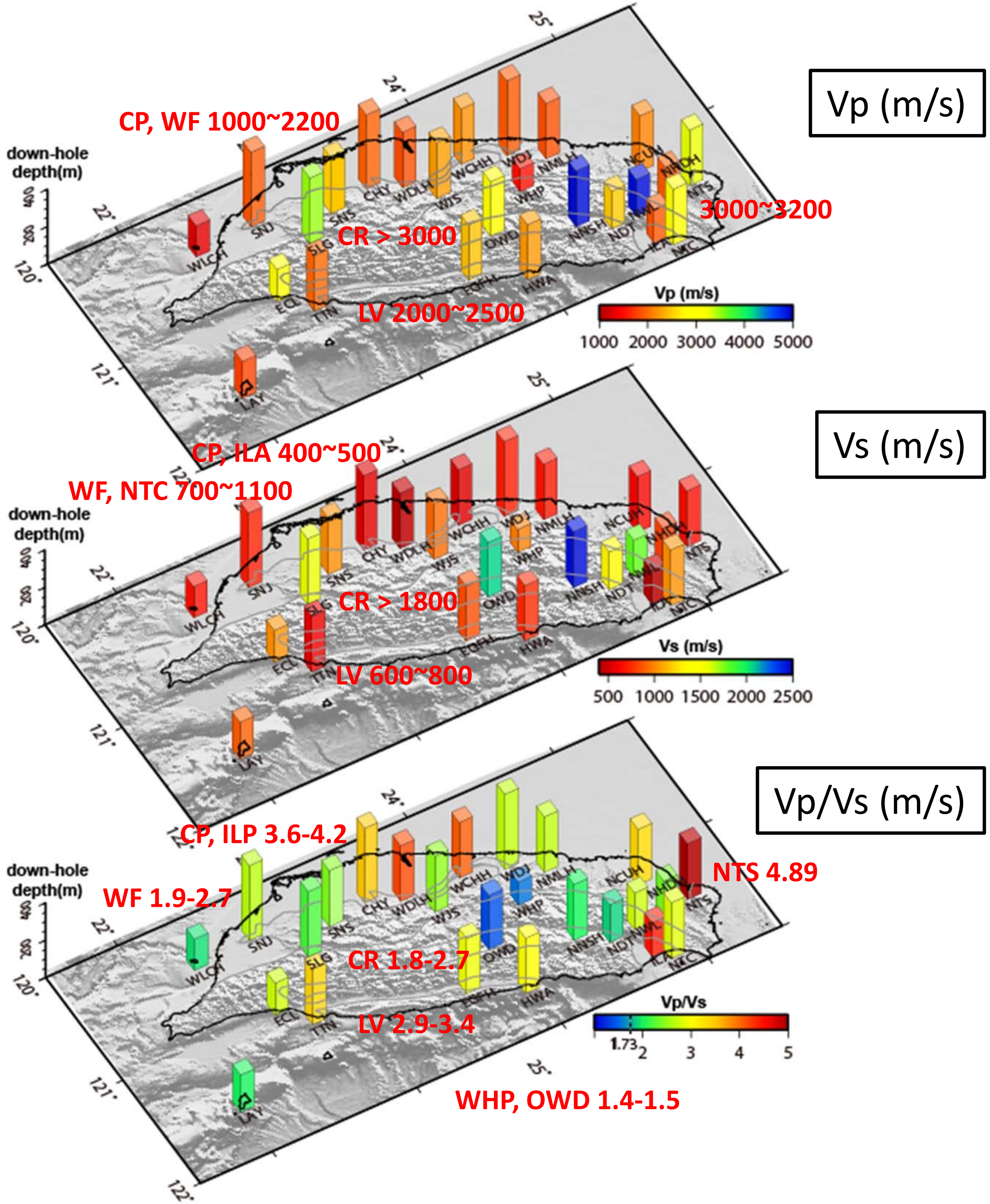
Vp (m/s)
CP, WF 1000~2200
down-hole depth(m)
CR > 3000
3000~3200
LV 2000~2500
Vp (m/s)
1000 2000 3000 4000 5000
Vs (m/s)
CP, ILA 400~500
WF, NTC 700~1100
down-hole depth(m)
CR > 1800
LV 600~800
Vs (m/s)
500 1000 1500 2000 2500
Vp/Vs (m/s)
CP, ILP 3.6-4.2
WF 1.9-2.7
down-hole depth(m)
NTS 4.89
CR 1.8-2.7
LV 2.9-3.4
Vp/Vs
1.73 2 3 4 5
WHP, OWD 1.4-1.5

Qp

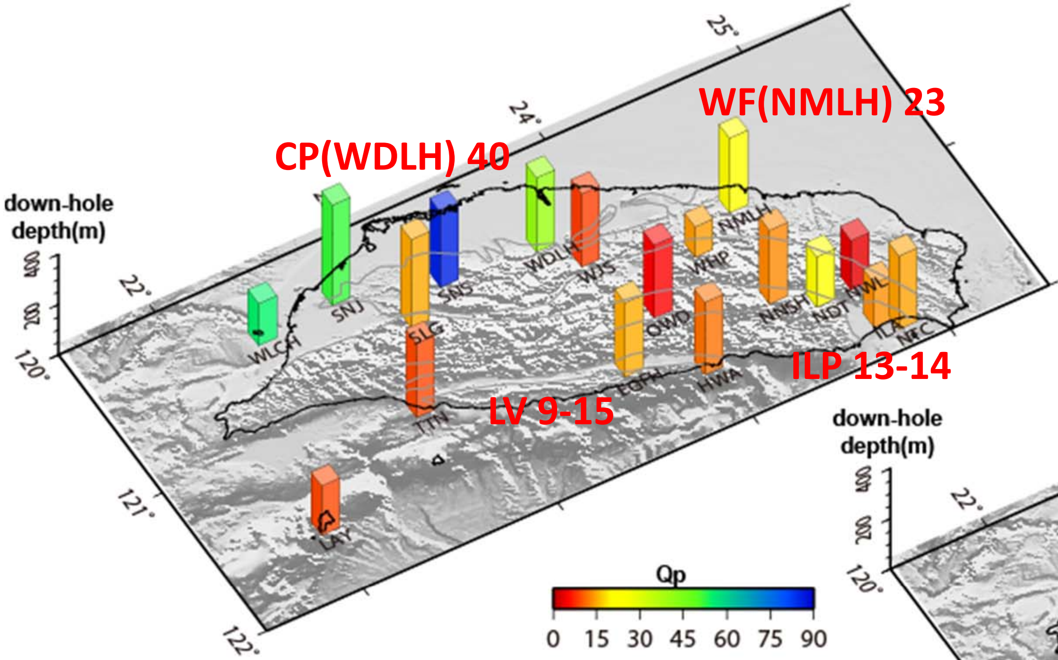

Qs

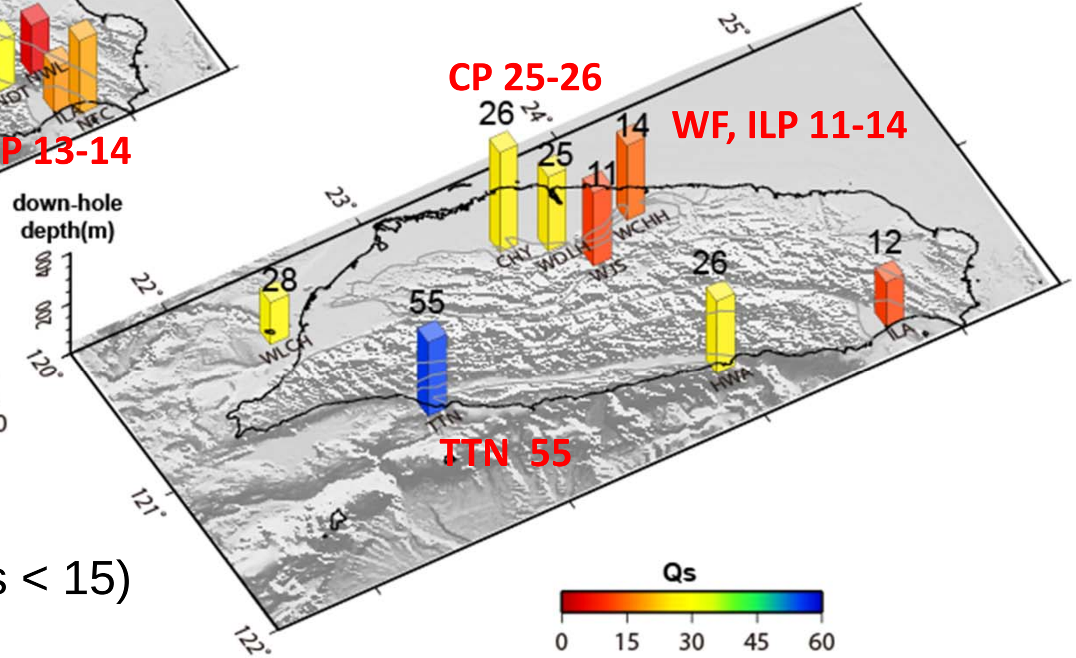

- Qp of 18 sites: 0~90 (most sites < 15)
- Maximum Qp : 86 (SNS)；
- Minimum Qp: 3.5-4.9 (NWL、OWD)
- CR Qp: 5~15 (NDT 24), lower than WF

Low Qp in CR ~ area of high thermal heat flow

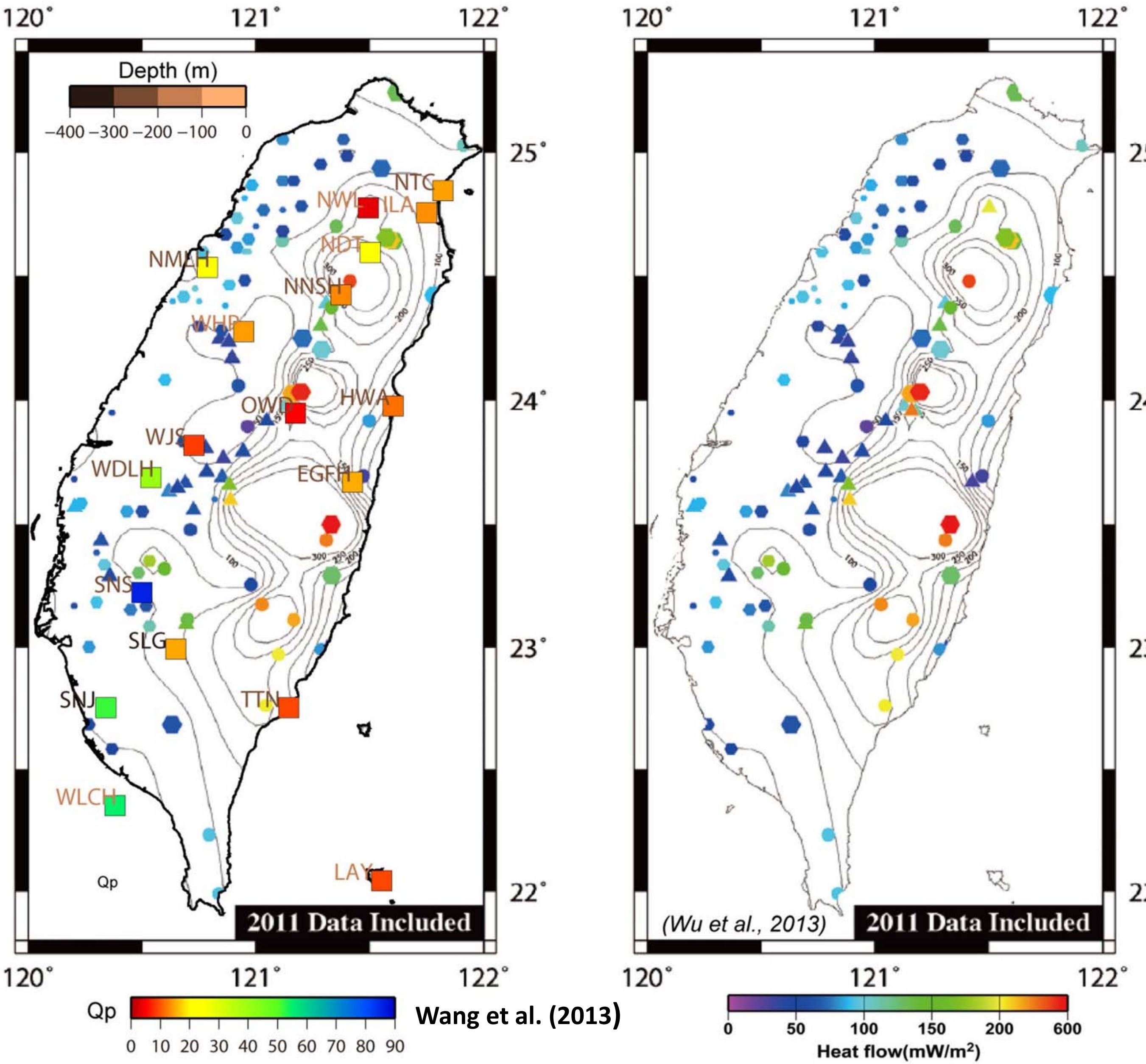

Attenuation applied in seismic engineering

Strong ground motion prediction

① Ground motion simulation

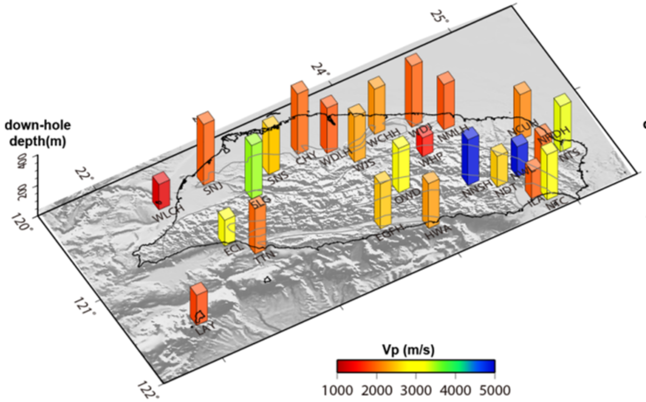

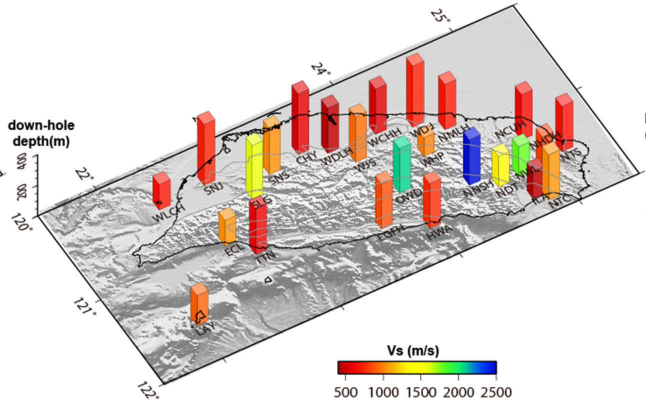

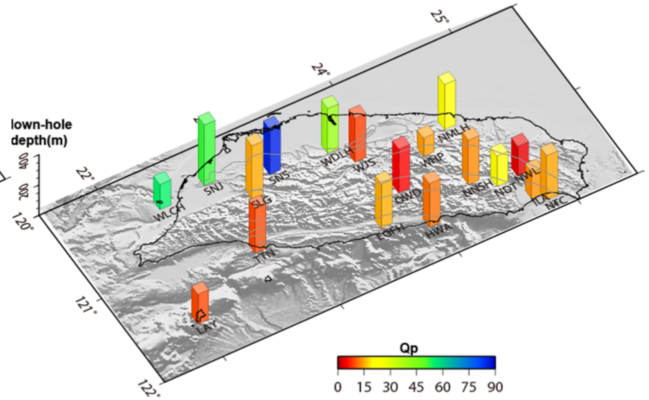

② Ground Motion Prediction Equation (GMPE)

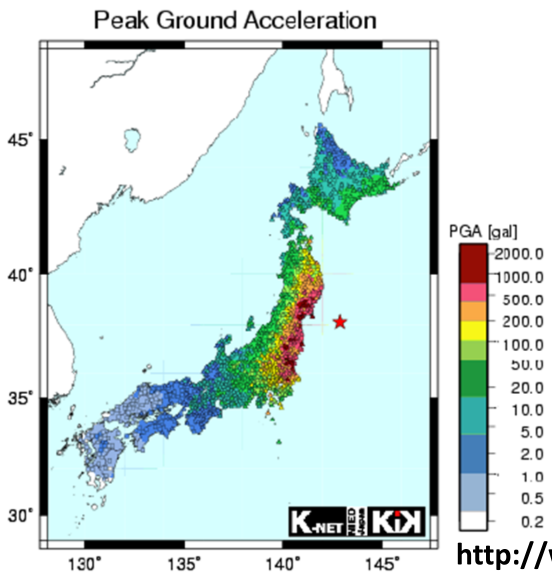

http://www.eri.u-tokyo.ac.jp..

.....

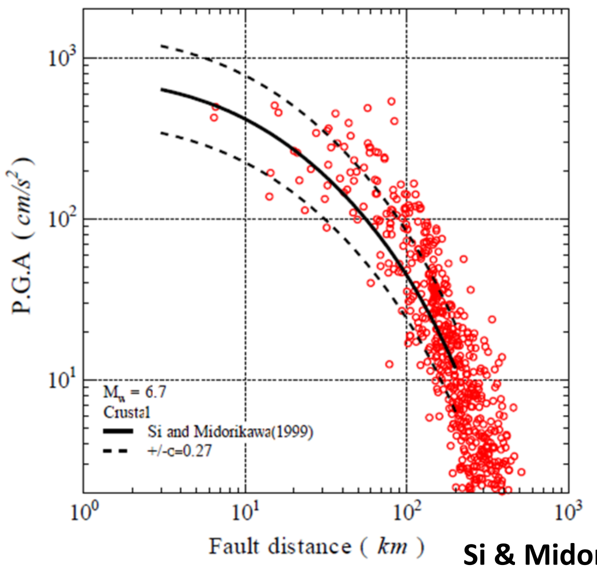

Si & Midorikawa (1999)

PGA & PGV compared with GMPEs of NGA2008

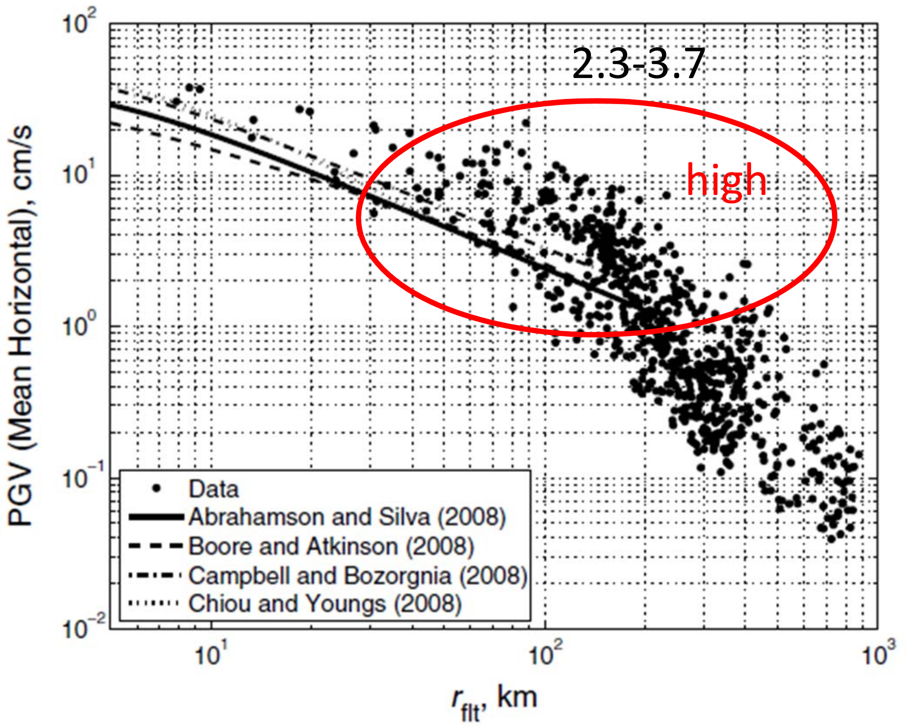

Figure 5. PGV compared with four different GMPEs. Curves assume $V_{S30} = 400$ m/s, as explained in the text.

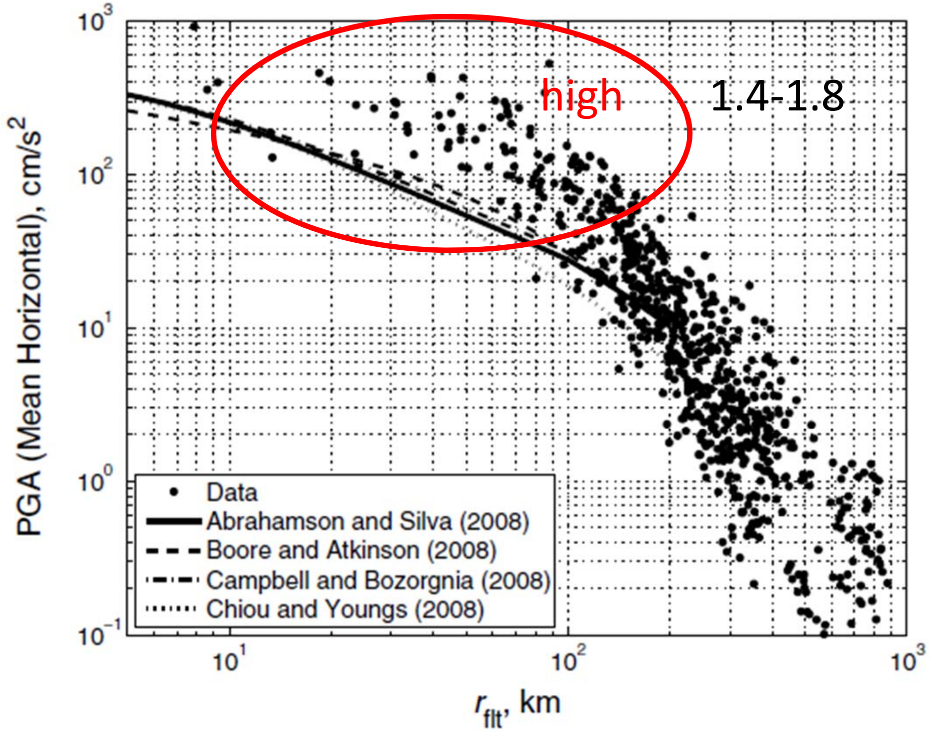

Figure 4. PGA, compared with four different GMPEs. Curves assume $V_{S30} = 400$ m/s, as explained in the text.

- A different choice of Vs30 can not help significantly to reduce the discrepancy.

Anderson et al. (2013)

Normal faulting events:

BATS (1995-2013)
Mw>4.0
Rake:-60~-90
recorded by at least 20 station
Total events:13
Total records:1067

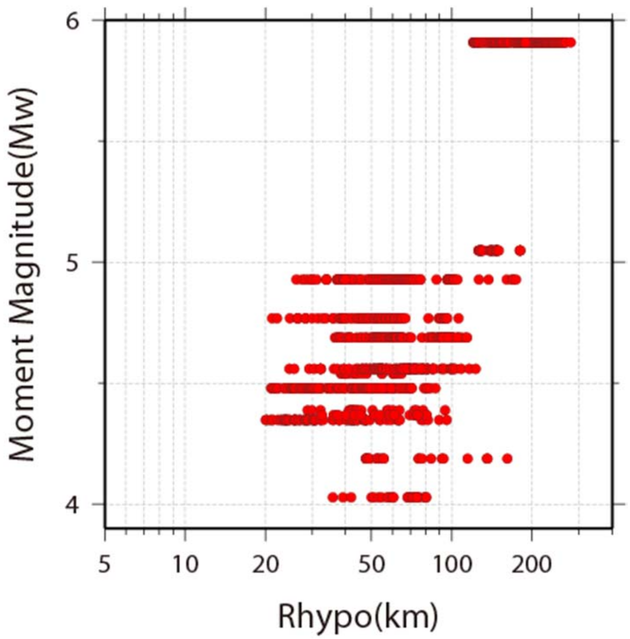

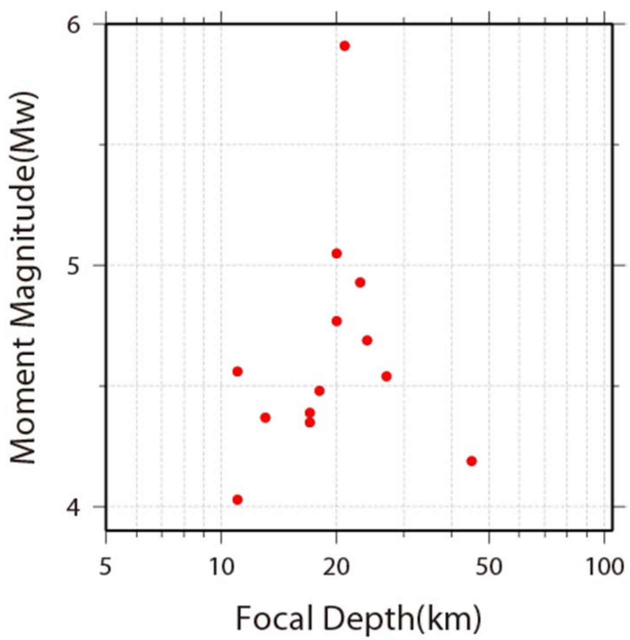

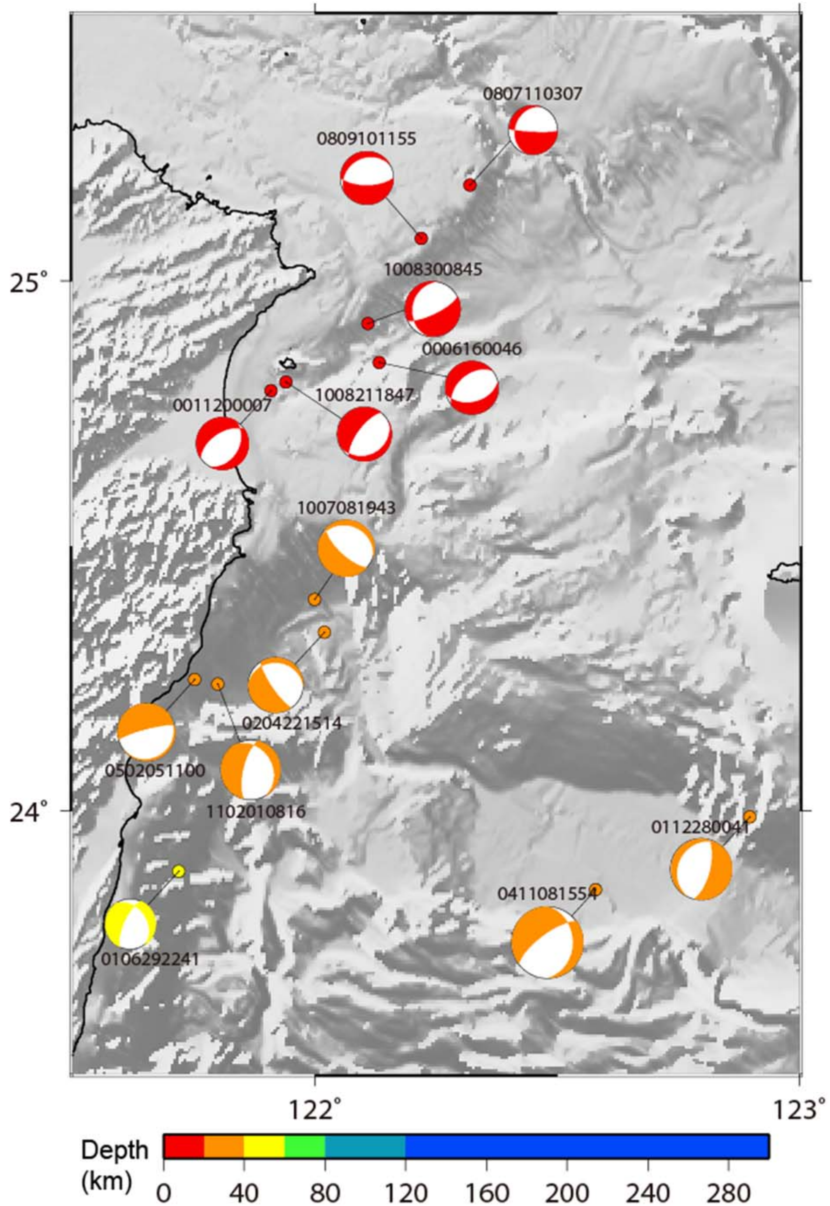

TSMIP Data → baseline correction filter → Pseudo-absolute acceleration response spectrum

Attenuation model I (Case1):

$$\rightarrow \ln(PGA\ or\ Sa) = C_1 + C_2 Mw + C_3 \ln\left(R_{hypo} + C_4 e^{c_5 Mw}\right) + C_6 H_i + C_7 * \ln(Vs_{30}/1130)$$

(Lin 2011, INER report)

Attenuation model II (Case 3):

$$\rightarrow \ln(PGA\ or\ Sa) = C_1 + C_2(Mw - 6.3) + C_3(8.5 - Mw)^2 + (C_4 + C_5(Mw - 6.3))\ln\left(\sqrt{R_{hypo}{}^2 + (e^H)^2}\right) + C_6 \ln(Vs_{30}/1130)$$

(Lin, 2009)

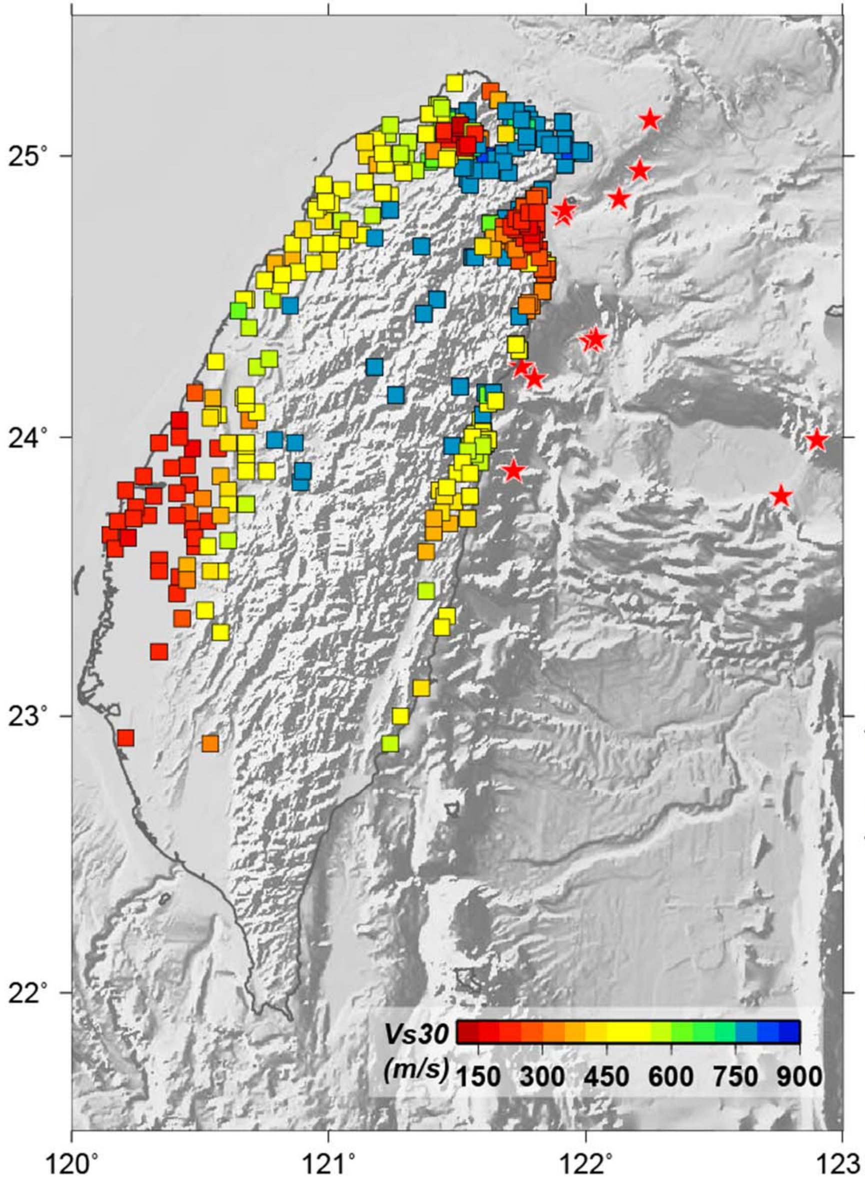

(Vs30 from Lee & Tsai, 2008)

1067 records :
Vs30 range: 110~835 (m/s)

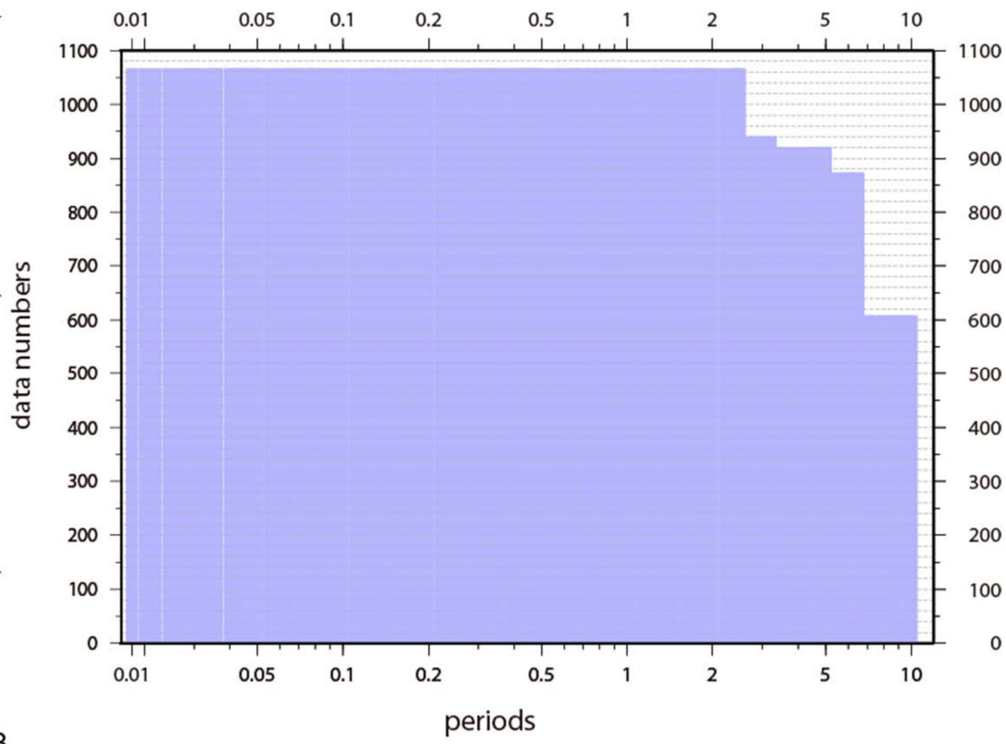

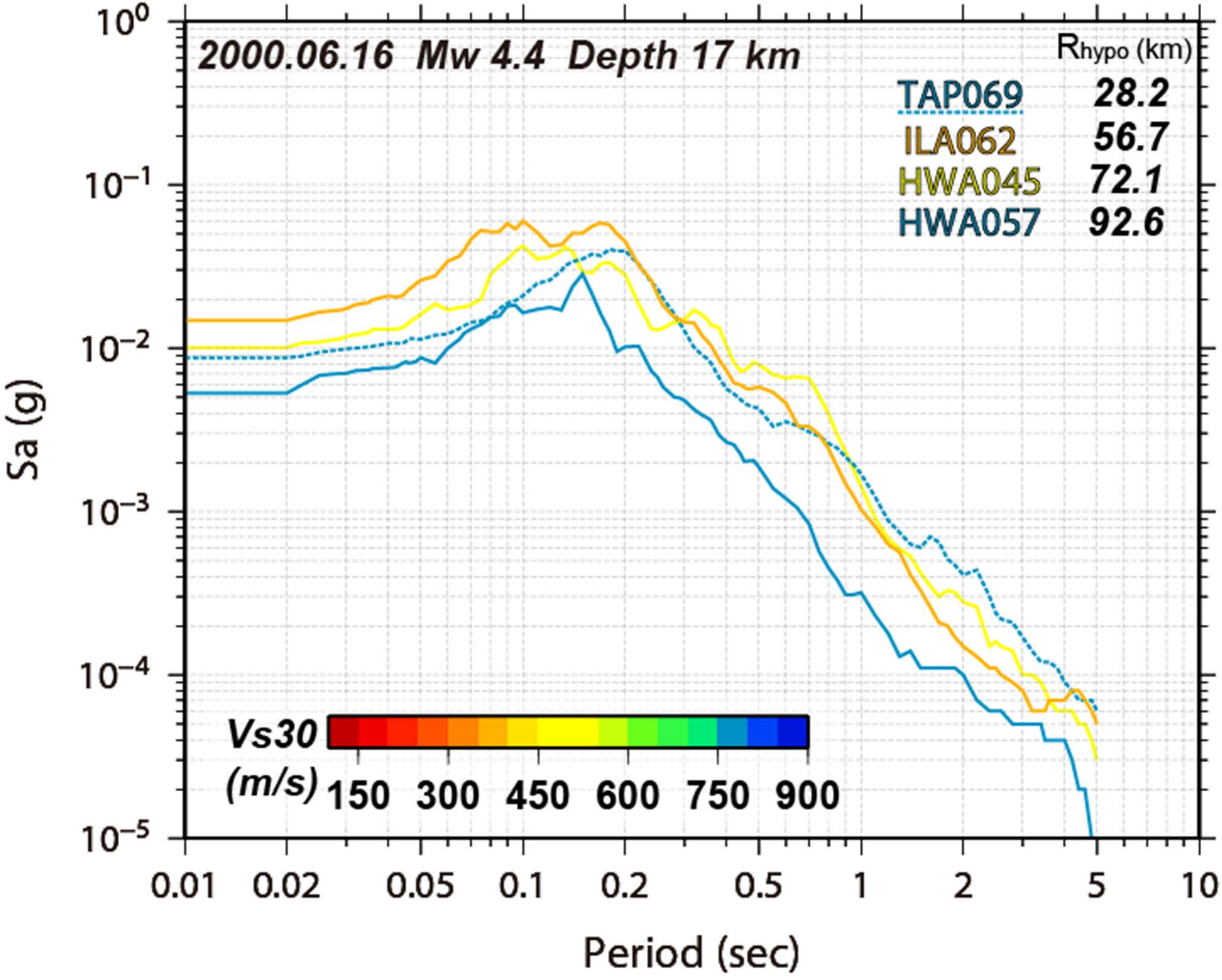

2000.06.16 Mw 4.4 Depth 17 km
Rhypo (km)
TAP069 28.2
ILA062 56.7
HWA045 72.1
HWA057 92.6
Vs30 (m/s)
150 300 450 600 750 900
Sa (g)
Period (sec)

2011.02.01 **Discrepancy between Case1 & Case3 : hypocentral distance < 20 km → simulation**

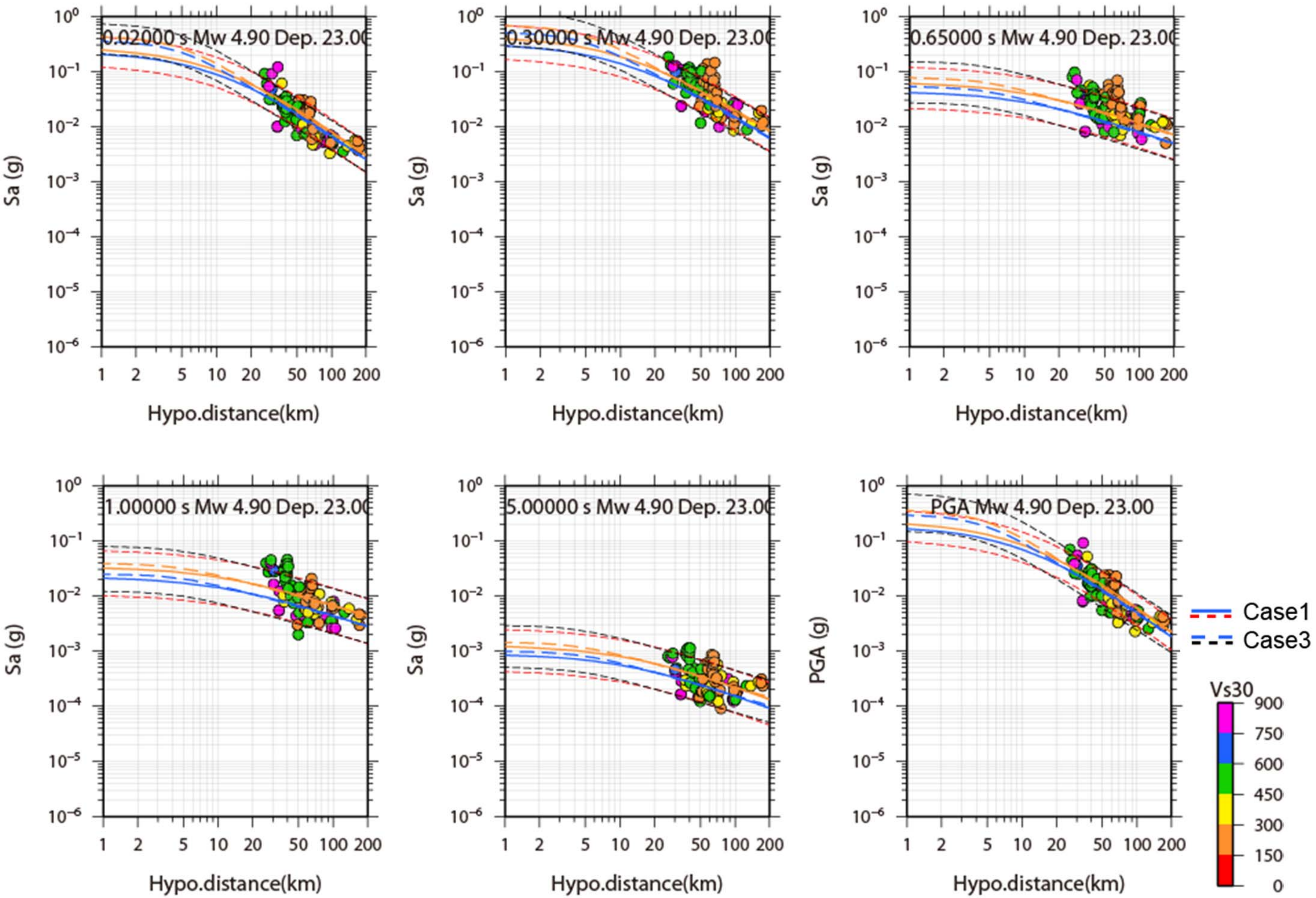

Comparison with data recorded by less than 20 stations

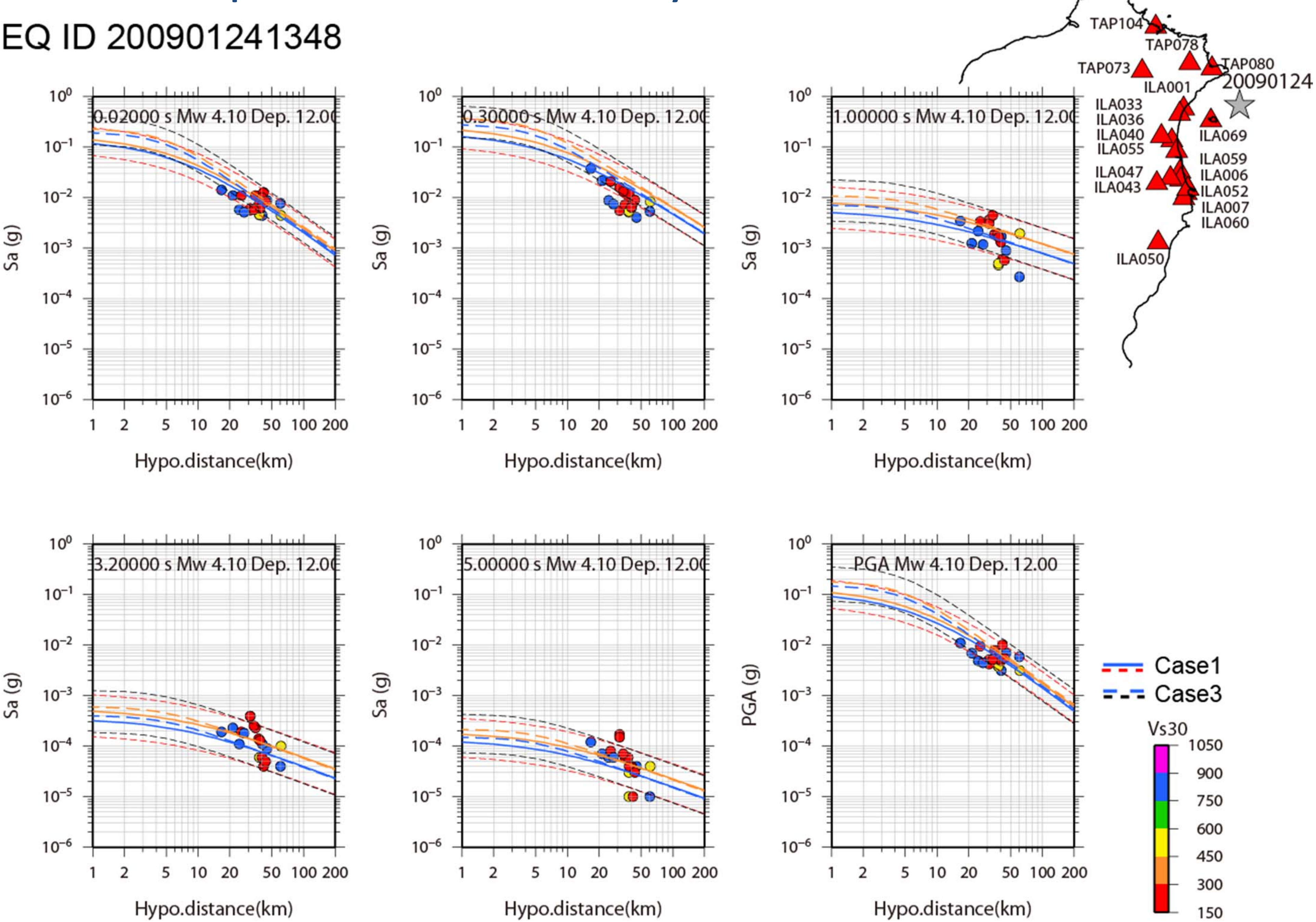

2010.08.30 08:45 Mw 4.6 Dep. 11km

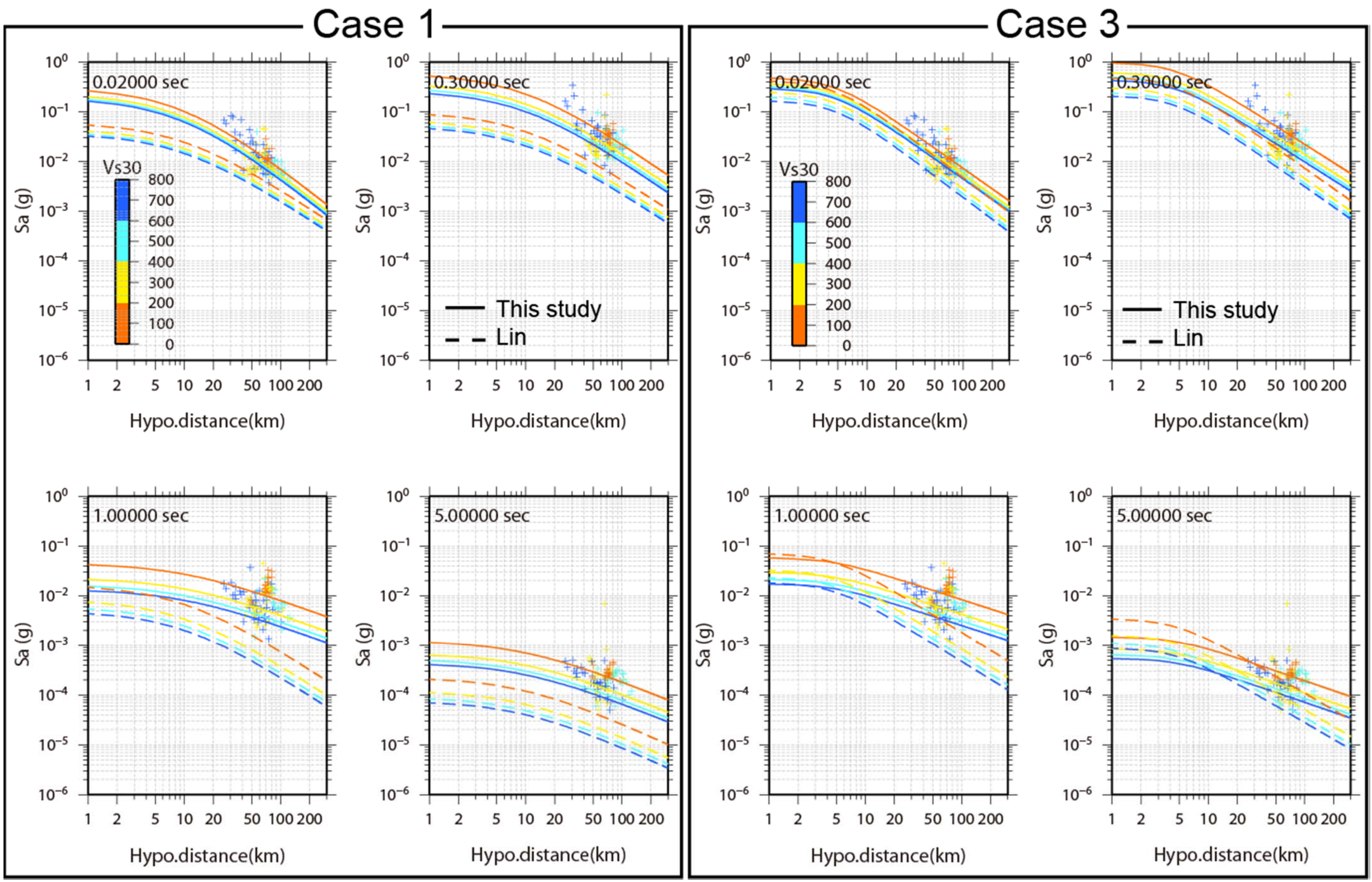

Normal faulting earthquake generates stronger Sa.

2010.08.30 08:45 Mw 4.6 Dep. 11km

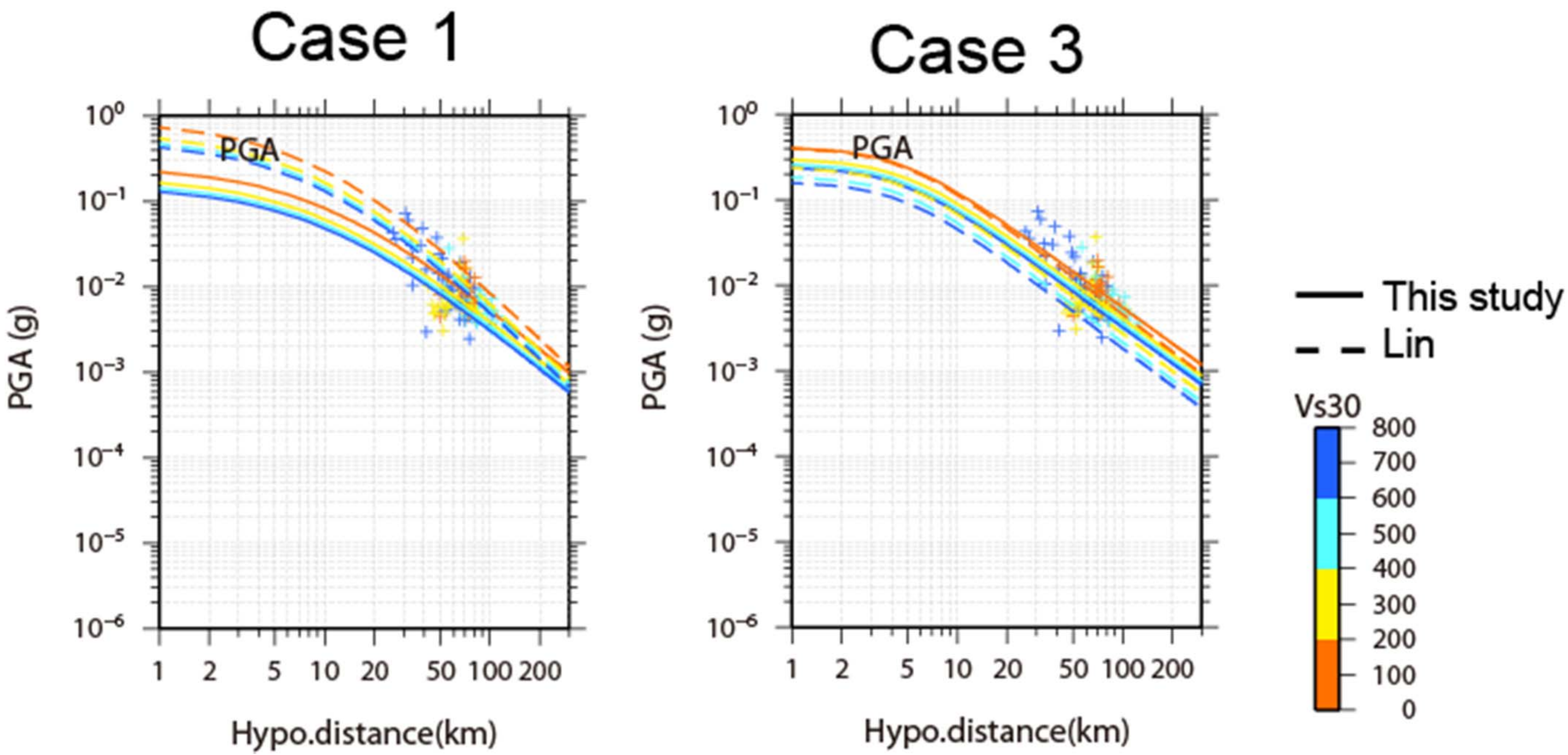

No difference between equations with and without considering fault mechanism.

The new GMPE for PGA do not reveal higher values for normal faulting earthquakes with Mw 4~6.

summaries

* The ***spatial variation in Qp-, and Qs-*** tomography reflect several prominent tectonic structural features and the structure heterogeneity bounded by the ***fault systems***, ex. ***Chelungpu Fault, Pingtung Plain***.

* The ***low Qp and Qs*** beneath the ***Central Range*** coincides well with the observed ***aseismic zone***, and imaged ***high temperature***. The low Q feature might be related to the high thermal extension resulted from ***lower crust exhumation*** during collision process.

* The significantly ***low Qp and low Qs*** within the Chelungpu fault zone was attributed to the ***existence of fluid, fracture and crack***.

* The ***high heat flow*** area in the Central Range exhibits ***low Qp*** values of the subsurface Qp model.

* The resultant attenuation relationship shows that the normal faulting earthquake generates ***stronger Sa*** which is not adopted for attenuation equation that usually used in Taiwan. The new GMPE for ***PGA do not reveal higher values*** for normal faulting earthquakes with Mw 4~6.

FIN

Thank you for your attention~